FERMILAB-CONF-18-498-AE-PPD

Year two instrument status of the SPT-3G cosmic microwave background receiver

A. N. Bender[a,b], P. A. R. Ade[c], Z. Ahmed[d,e], A. J. Anderson[f,b], J. S. Avva[g], K. Aylor[h], P. S. Barry[b], R. Basu Thakur[b], B. A. Benson[f,b,i], L. S. Bleem[a,b], S. Bocquet[j,a], K. Byrum[a], J. E. Carlstrom[b,k,l,a,i], F. W. Carter[a,b], T. W. Cecil[a], C. L. Chang[a,b,i], H.-M. Cho[e], J. F. Cliche[m], T. M. Crawford[b,i], A. Cukierman[g], T. de Haan[g], E. V. Denison[n], J. Ding[o], M. A. Dobbs[m,p], S. Dodelson[q], D. Dutcher[b,l], W. Everett[r], A. Foster[s], J. Gallicchio[b,t], A. Gilbert[m], J. C. Groh[g], S. T. Guns[g], N. W. Halverson[r,u], A. H. Harke-Hosemann[v,a], N. L. Harrington[g], J. W. Henning[a,b], G. C. Hilton[n], G. P. Holder[m,p,w], W. L. Holzapfel[g], N. Huang[g], K. D. Irwin[d,x,e], O. B. Jeong[g], M. Jonas[f], T. S. Khaire[o], L. Knox[h], A. M. Kofman[v], M. Korman[s], D. L. Kubik[f], S. Kuhlmann[a], C.-L. Kuo[d,x,e], A. T. Lee[g,y], E. M. Leitch[b,i], A. E. Lowitz[b], S. S. Meyer[b,k,l,i], D. Michalik[z], J. Montgomery[m], A. Nadolski[v], T. Natoli[aa], H. Ngyuen[f], G. I. Noble[m], V. Novosad[o], S. Padin[b], Z. Pan[b,l], J. Pearson[o], C. M. Posada[o], W. Quan[b,l], S. Raghunathan[bb], A. Rahlin[f,b], C. L. Reichardt[bb], J. E. Ruhl[s], J.T. Sayre[r], E. Shirokoff[b,i], G. Smecher[cc], J. A. Sobrin[b,l], A. A. Stark[dd], K. T. Story[d,x], A. Suzuki[y], K. L. Thompson[d,x,e], C. Tucker[c], L. R. Vale[n], K. Vanderlinde[aa,ee], J. D. Vieira[v,w], G. Wang[a], N. Whitehorn[ff,g], W. L. K. Wu[b], V. Yefremenko[a], K. W. Yoon[d,x,e], and M. R. Young[ee]

[a]High-Energy Physics Division, Argonne National Laboratory, 9700 South Cass Avenue., Argonne, IL, USA 60439
[b]Kavli Institute for Cosmological Physics, University of Chicago, 5640 South Ellis Avenue, Chicago, IL, USA 60637
[c]School of Physics and Astronomy, Cardiff University, Cardiff CF24 3YB, United Kingdom
[d]Kavli Institute for Particle Astrophysics and Cosmology, Stanford University, 452 Lomita Mall, Stanford, CA, USA 94305
[e]SLAC National Accelerator Laboratory, 2575 Sand Hill Road, Menlo Park, CA, USA 94025
[f]Fermi National Accelerator Laboratory, MS209, P.O. Box 500, Batavia, IL, USA 60510
[g]Department of Physics, University of California, Berkeley, CA, USA 94720
[h]Deptartment of Physics, University of California, One Shields Avenue, Davis, CA 95616
[i]Department of Astronomy and Astrophysics, University of Chicago, 5640 South Ellis Avenue, Chicago, IL, USA 60637
[j]Ludwig-Maximilians-Universität, Scheiner- str. 1, 81679 Munich, Germany
[k]Enrico Fermi Institute, University of Chicago, 5640 South Ellis Avenue, Chicago, IL, USA 60637
[l]Department of Physics, University of Chicago, 5640 South Ellis Avenue, Chicago, IL, USA 60637
[m]Department of Physics, McGill University, 3600 Rue University, Montreal, Quebec H3A 2T8, Canada
[n]NIST Quantum Devices Group, 325 Broadway Mailcode 817.03, Boulder, CO, USA 80305
[o]Materials Sciences Division, Argonne National Laboratory, 9700 South Cass Avenue, Argonne, IL, USA 60439
[p]Canadian Institute for Advanced Research, CIFAR Program in Cosmology and Gravity, Toronto, ON, M5G 1Z8, Canada
[q]Department of Physics, Carnegie Mellon University, Pittsburgh, Pennsylvania, USA 15312

This document was prepared by South Pole Telescope collaboration using the resources of the Fermi National Accelerator Laboratory (Fermilab), a U.S. Department of Energy, Office of Science, HEP User Facility. Fermilab is managed by Fermi Research Alliance, LLC (FRA), acting under Contract No. DE-AC02-07CH11359.

[r]CASA, Department of Astrophysical and Planetary Sciences, University of Colorado, Boulder, CO, USA 80309
[s]Department of Physics, Center for Education and Research in Cosmology and Astrophysics, Case Western Reserve University, Cleveland, OH, USA 44106
[t]Harvey Mudd College, 301 Platt Boulevard., Claremont, CA, USA 91711
[u]Department of Physics, University of Colorado, Boulder, CO, USA 80309
[v]Department of Astronomy, University of Illinois at Urbana-Champaign, 1002 West Green Street, Urbana, IL, USA 61801
[w]Department of Physics, University of Illinois Urbana-Champaign, 1110 West Green Street, Urbana, IL, USA 61801
[x]Deptartment of Physics, Stanford University, 382 Via Pueblo Mall, Stanford, CA, USA 94305
[y]Physics Division, Lawrence Berkeley National Laboratory, Berkeley, CA, USA 94720
[z]University of Chicago, 5640 South Ellis Avenue, Chicago, IL, USA 60637
[aa]Dunlap Institute for Astronomy & Astrophysics, University of Toronto, 50 St. George Street, Toronto, ON, M5S 3H4, Canada
[bb]School of Physics, University of Melbourne, Parkville, VIC 3010, Australia
[cc]Three-Speed Logic, Inc., Vancouver, B.C., V6A 2J8, Canada
[dd]Harvard-Smithsonian Center for Astrophysics, 60 Garden Street, Cambridge, MA, USA 02138
[ee]Department of Astronomy & Astrophysics, University of Toronto, 50 St. George Street, Toronto, ON, M5S 3H4, Canada
[ff]Department of Physics and Astronomy, University of California, Los Angeles, CA, USA 90095

ABSTRACT

The South Pole Telescope (SPT) is a millimeter-wavelength telescope designed for high-precision measurements of the cosmic microwave background (CMB). The SPT measures both the temperature and polarization of the CMB with a large aperture, resulting in high resolution maps sensitive to signals across a wide range of angular scales on the sky. With these data, the SPT has the potential to make a broad range of cosmological measurements. These include constraining the effect of massive neutrinos on large-scale structure formation as well as cleaning galactic and cosmological foregrounds from CMB polarization data in future searches for inflationary gravitational waves. The SPT began observing in January 2017 with a new receiver (SPT-3G) containing ∼16,000 polarization-sensitive transition-edge sensor bolometers. Several key technology developments have enabled this large-format focal plane, including advances in detectors, readout electronics, and large millimeter-wavelength optics. We discuss the implementation of these technologies in the SPT-3G receiver as well as the challenges they presented. In late 2017 the implementations of all three of these technologies were modified to optimize total performance. Here, we present the current instrument status of the SPT-3G receiver.

1. INTRODUCTION

The South Pole Telescope (SPT) is 10-meter telescope surveying the millimeter-wavelength sky from the geographic South Pole (see Figure 1).[1] Since its initial commissioning in 2007, the SPT has hosted three instruments designed to make high resolution maps of the cosmic microwave background (CMB). The CMB intensity and polarization data from SPT-SZ and SPTpol have been used for a number of cosmological and astrophysical studies. These include measurements of the CMB power spectrum damping tail,[2,3] reconstructing maps of CMB gravitational lensing for large-scale structure (LSS) studies,[4–6] and searching for galaxy clusters[7,8] and millimeter-wavelength transient events.[9]

Send correspondence to A. N. Bender: abender@anl.gov

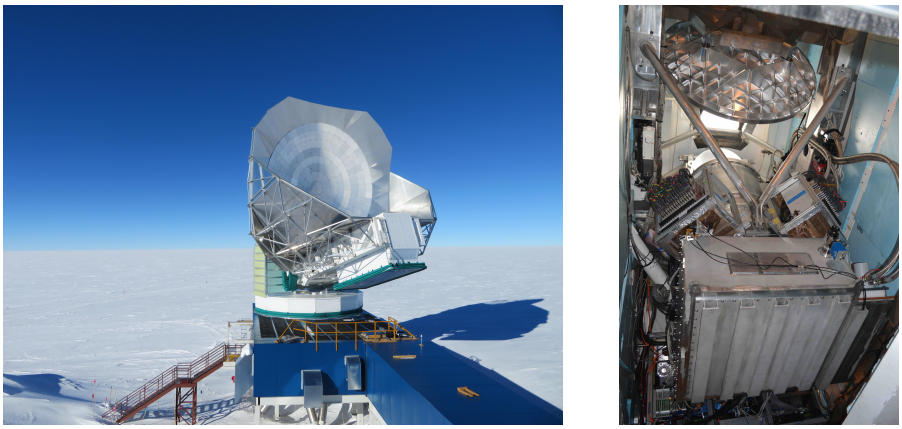

Figure 1. *Left:* The South Pole telescope. The 10-meter primary dish is surrounded by reflective baffles to prevent ground contamination. The SPT-3G receiver is installed in the telescope boom shown protruding off the front of the dish. *Right:* The SPT-3G cryogenic receiver installed in the telescope boom. The back side of the secondary mirror is shown in the upper part of the picture. Cryogenic optics are housed in the cylindrical portion of the receiver and the detectors in the rectangular bottom portion. Also shown are the two crates of readout electronics used to operate the detectors.

SPTpol was replaced with the SPT-3G receiver in late 2016. The SPT-3G receiver observes at 95, 150, and 220 GHz with polarization sensitivity and is a significantly more sensitive instrument than SPTpol. All three SPT instruments use superconducting detectors that are uniquely sensitive due to their ability to operate in the photon-noise dominated regime. The SPT-3G focal plane hosts 16,140 of these detectors, an order of magnitude more than SPT-SZ or SPTpol. With this state-of-the-art focal plane, SPT-3G is opening a new regime in high-precision measurements of the CMB polarization.

The SPT-3G receiver is now in its second year of operation. A summary of on-sky performance from the initial commissioning of the instrument can be found elsewhere.[10–12] During the austral summer of 2017-2018 several key changes were made to the receiver to improve total instrumental sensitivity. These improvements included new broadband anti-reflection coatings on the optics, optimized detector thermal properties, and modifications to the readout electronics to reduce noise. Here, we discuss the current performance and status of SPT-3G after the successful implementation of those improvements. The structure of the paper is as follows. In Section 2, we briefly review the cosmological physics that SPT-3G probes using observations of the CMB. Section 3 describes key features of the instrument design and the improvements made to the receiver for the 2018 observing season. The overall performance of the SPT-3G receiver is discussed in Section 4 and cosmological forecasts are presented in Section 5.

2. SCIENTIFIC GOALS

The SPT-3G receiver measures both the intensity and polarization of the CMB with exceptional sensitivity at a broad range of angular scales on the sky. Here, we briefly review the cosmological physics targeted by SPT-3G.[13] Using the CMB polarization, SPT-3G will probe fundamental physics in both the early and late universe. The CMB is intrinsically polarized from the Thomson scattering of photons directly prior to recombination. The resulting polarization pattern exhibits even-parity (i.e., it is curl-free), and is referred to as the *E-mode* polarization.[14] The CMB E modes originate from the same primary anisotropies seen in the intensity, therefore, they provide a semi-independent probe of the base cosmological model, known as ΛCDM . Precise constraints on the ΛCDM model are well-motivated as hints of tension between local probes and the CMB have surfaced.[3,15] While these discrepancies might be resolved through unaccounted for instrumental or astrophysical systematics, they could also be pointing towards new physics beyond ΛCDM. New and independent data sets such as those from SPT-3G have the potential to resolve or widen these cracks.

The polarization of the CMB also contains an odd-parity component, known as the *B modes*.[16] As the CMB traverses through the universe, the light is gravitationally lensed by the structure that it encounters. The lensing

introduces a curl into the polarization pattern, transforming E-mode polarization into B-mode polarization. The amplitude of the lensing B-mode signal is proportional to the amount of LSS in the universe, providing a probe of physics that influences LSS growth, including massive neutrinos. Additionally, gravitational waves from an inflationary epoch imprint a B-mode polarization pattern in the CMB. Detection of this signal would provide extremely compelling evidence in support of inflation, as well as constraining its energy scale. Measurements of primordial gravitational waves are parameterized in terms of r (the tensor to scalar ratio), which corresponds to the amplitude of the B-mode signal. Inflationary B modes are undetected at this point in time with the most stringent upper limit placed by BICEP2/Keck of $r < 0.07$ at 95% confidence.[17]

Measurements of the polarization of the CMB, and particularly the B modes, will provide significant breakthroughs in our fundamental understanding of both inflation and the neutrino sector. There are, however, three sizeable barriers to achieving these landmark measurements. First, the gravitational lensing B-mode polarization signal is roughly four to five orders of magnitude fainter than the CMB intensity anisotropies and the primordial signal is constrained to be even smaller. A significant leap in instrumental sensitivity is required to improve on current measurements. Second, galactic foregrounds confuse the CMB signal with both synchrotron and dust components.[18,19] Observations at multiple frequencies are necessary to perform component separation. Finally, the gravitational lensing B modes occur mostly on small angular scales and the inflationary B-mode signal is at larger angular scales. However, there is a significant region of overlap where the lensing B modes are essentially a foreground for the inflationary signal. Cleaning the lensing B modes from the data (a process called delensing) will be critically important in improving on current constraints on inflationary B modes.[20,21] The SPT-3G instrument is designed with all three of these challenges in mind. The large-format focal plane has an order of magnitude more detectors than SPTpol, significantly increasing instrumental sensitivity. SPT-3G observes at three different frequency bands to facilitate component separation between the CMB and galactic foregrounds. Lastly, SPT-3G maps the CMB with high resolution. These data will result in a high signal-to-noise measurement of the gravitational lensing B modes and their use in the delensing process.

In addition to the cosmological signals discussed above, the high resolution of the SPT enables scientific studies involving detection of galaxies and galaxy clusters. Clusters of galaxies are detected through the scattering of CMB photons off hot (keV) electrons in the intracluster medium, known as the Sunyaev-Zel'dovich effect (SZE).[22] Because the SZE is a scattering effect it does not suffer from the cosmological dimming that makes x-ray and optical observations of high-redshift clusters challenging. The resulting sample of galaxy clusters from SPT-3G will be nearly mass-limited and extend over a wide range of redshifts. The clusters serve as a tracer of the evolution of LSS in the universe and thus a probe of neutrino mass and dark energy.[23] SPT-3G will also detect high-redshift dusty star-forming galaxies, which will be used in studies of galaxy formation in the early universe.[24]

3. THE SPT-3G INSTRUMENT

The SPT-3G instrument is designed to couple the maximum number of detectors to the sky allowed by the existing SPT primary mirror and receiver cabin. The instrument consists of an optical chain of both mirrors and lenses, a focal plane of detectors, and the associated readout electronics. Each component has unique requirements and challenges, which are briefly summarized in the following sections. The SPT-3G instrument was installed into the telescope in early 2017 and spent the first year of operations focused on commissioning and calibration.[10,11] Based on the results of these data, three improvements to the receiver in the areas of optics, detectors, and readout were implemented. The motivation and features of these improvements are discussed below.

3.1 Optics

The SPT-3G instrument couples light from the 10-meter primary mirror to the detectors using a set of wide-field broadband optics.[13,25] An ellipsoidal secondary and flat tertiary mirror (both at ambient temperature) direct the light from the primary dish through a window into the optics section of the receiver cryostat (see Figure 2). From there the light passes through an alumina plate that provides support for the vacuum window and three large (720 mm diameter) cryogenic alumina lenses. Additionally, there is a 280 mm Lyot stop which reduces the illumination of the primary mirror to the inner eight meters. The optical configuration results in a 1.9 degree field-of-view and a large 43 cm diameter image plane. Hemispherical alumina lenslets couple the microwave light

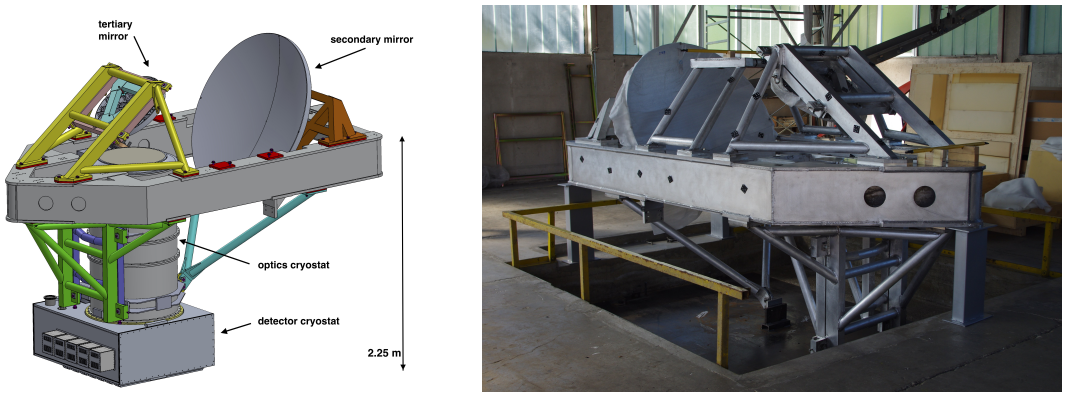

Figure 2. *Left:* A CAD drawing of the SPT-3G optics and cryogenic receiver configuration. *Right:* The SPT-3G optics bench, including the secondary and tertiary mirrors.

from the image plane into antennas in the detector array. With diffraction-limited performance, a beam size of 1.6/1.2/1.1 arcminutes is measured at 95/150/220 GHz, respectively.

The wide-field design of the SPT-3G optics enables the packing of 16,140 detectors into the focal plane and a high array sensitivity compared to its predecessors. In addition to this wide field, a second key consideration in the optics design is to ensure high optical transmission across the 95, 150, and 220 GHz observation bands. Transmission at the surface of each optical element directly impacts total instrumental sensitivity. The vacuum window is made from annealed HDPE, which is both highly transparent to microwave radiation and strong enough to support the approximately 12,000 pound load from the atmosphere. Instead of an antireflection coating, 1.321 mm tall triangular grooves spaced at 0.609 mm intervals are machined into each side of the window. The grooves are orthogonal on opposite sides of the window to eliminate any net polarization rotation. A previous implementation of a similar groove geometry resulted in excellent transmission at the relevant wavelengths[26] and 95% transmission was verified using a fourier transform spectrometer.

The alumina lenses and window backing plate are anti-reflection (AR) coated to minimize reflections at these surfaces, increasing total transmission and minimizing thermal loading from stray light scattering inside the receiver. For the initial deployment of SPT-3G, the large lenses had a two-layer coating optimized for the 95/150 GHz bands that was applied using plasma spray technology.[27] Due to challenges encountered with the performance of the third layer (220 GHz) at cryogenic temperatures the AR coating technology was updated for the second year of operation. New lenses with a three-layer polytetrafluoroethylene-based (PTFE) coating were manufactured and installed.[25] The alumina lenslets (shown in the left panel of Figure 3) are also AR coated with three layers of PTFE.

3.2 Detectors

The SPT-3G focal plane contains pixels that are sensitive to both orthogonal linear polarizations in three observing bands (95/150/220 GHz). Each pixel contains six individual detectors to measure these signals. Microwave radiation is absorbed by a broadband sinuous antenna, measuring both polarizations simultaneously in perpendicular arms and then directing the power onto separate microstrip lines.[28] The power is further separated by observing band using an in-line triplexing filter and then deposited onto transition-edge sensor (TES) bolometers. The TES is made of a quad-layer stack of titanium-gold-titanium-gold with an overall superconducting transition temperature $T_c \sim 420 - 480$ mK.[29] Additional details on the SPT-3G pixel design and its performance can be found in previous publications.[30–32] The detectors are fabricated on six-inch silicon wafers each containing 269 pixels (see the right hand panel of Figure 3). There are ten of the hexagonal detector wafers in the SPT-3G focal plane for a total of 16,140 TES bolometers. The detectors and a portion of the associated readout are cooled to a temperature of ∼280 mK using closed-cycle mechanical refrigerators.

The sensitivity with which a TES can map the sky is determined by its noise equivalent power (NEP). In the ideal photon-noise dominated limit, the intrinsic NEP of the TES itself and the NEP of the readout system

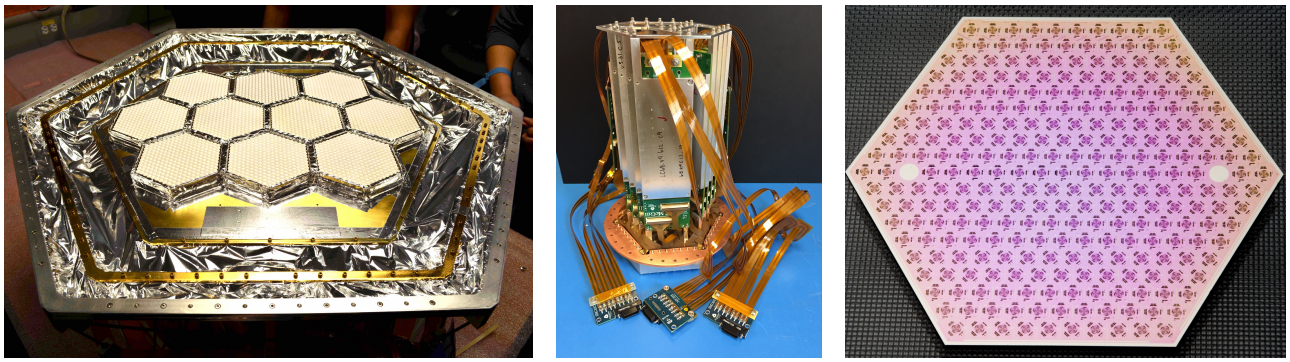

Figure 3. *Left:* The fully assembled SPT-3G focal plane. In the center are the ten hexagonal detector modules. The white hemispherical lenslets couple the microwave power to antennas below. Also shown is aluminized mylar that serves as an RF shield connecting between the different temperature stages of the focal plane structure. *Middle:* The backside of a single detector module with the millikelvin readout electronics (the *LC* filter networks) assembled onto the backplate. The long broadside-coupled striplines connect the module to the SQUID amplifiers. *Right:* An SPT-3G detector wafer with 269 pixels. Each of the ∼3 mm antennas is connected to and surrounded by six transition-edge sensor bolometers.

are subdominant to the fluctuations in arrival of the incoming microwave photons. The level of thermal carrier (phonon) noise in the TES is related to the saturation power ($P_{\rm sat}$, the amount of power required to drive the TES into a normal resistive state). The $P_{\rm sat}$ for the SPT-3G detectors has been optimized to reduce this noise contribution while still maintaining dynamic range and stability requirements. Beyond the improvement to the phonon noise, reducing $P_{\rm sat}$ reduces the electrical power and thus the voltage bias needed to operate the TES stably in the superconducting transition. The noise power contributed by the readout system is proportional to the voltage bias, therefore, optimized $P_{\rm sat}$ benefits the the readout noise as well (see Section 3.3).

In the first year of operation, the saturation powers in typical SPT-3G detectors were 17/22/25 pW for 95/150/220 GHz, respectively.[10] These values were higher than optimal due to uncertainty in the optical loading.[10,33] Additional detector wafers were fabricated targeting lower $P_{\rm sat}$ in all three bands. Ten new detector wafers (the full SPT-3G focal plane) were installed into the SPT-3G receiver for the second year of operation with a median $P_{\rm sat}$ of roughly 12/14/14 pW.[34]

3.3 Readout

The SPT-3G focal plane is read out using a frequency domain multiplexing (fMux) scheme.[35] Multiplexing is a key technology for large focal planes like SPT-3G because it reduces the thermal loading on the millikelvin stage due to readout wiring. In fMux, each TES bolometer is connected in series with an inductor and capacitor to assign it a unique resonant frequency. These elements are connected in parallel to create a network of resonant filters and detectors (see Figure 4). In this configuration a single pair of wires is used to apply a waveform of AC voltage biases (referred to as the *carriers*) to the bolometers and read out the subsequent signals. The *LC* filter selects the appropriate voltage bias for each detector in the network. In the SPT-3G focal plane, each module multiplexes 66 bolometers together with resonant frequencies between 1.6 and 5.2 MHz for a total of 240 readout modules.[36,37]

When microwave power from the sky is deposited onto the TES island the electrical resistance and current flowing through the TES changes in response. The resulting amplitude modulation of the AC voltage bias creates signals in the sidebands. The currents from all the TESs in a module are summed together and input into a Superconducting Quantum Interference Device (SQUID)[38] where they are amplified, converted to a voltage, and subsequently digitized. A process called digital active nulling (DAN)[39] removes both the carriers and the measured sky sideband signals from the current input into the SQUID (the *nuller* in Figure 4). When DAN is running the sideband signals in the nuller are the final measured sky signal.

The *LC* filter networks are constructed through similar micro-fabrication techniques as the TES detectors. Interdigitated capacitors and spiral inductors are patterned in a superconducting material (either aluminum or

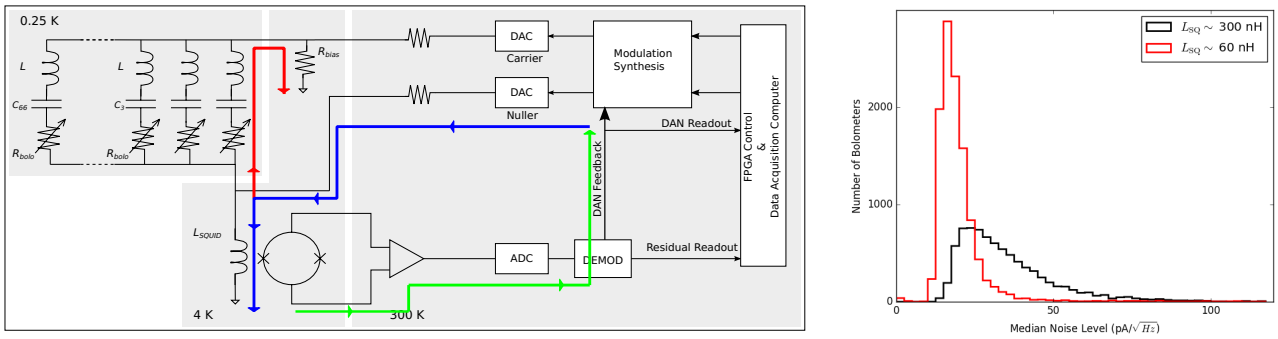

Figure 4. *Left:* A schematic diagram of the fMux readout system as implemented in SPT-3G. The blue and red arrows demonstrate the two possible paths that current can flow when injected by the nuller, creating an amplification of noise that couples into the system in the demodulation chain (green arrow, see text). *Right:* A comparison of SPT-3G noise performance when the bolometers are held above the superconducting transition temperature. The black curve shows the noise prior to the improvement in the filtering of signal waveforms output by the FPGA motherboard and the installation of SQUIDs with lower input impedance to mitigate demodulation noise amplification. The red histogram ($L_{\rm SQ} \sim 60$ nH) shows the current noise performance of SPT-3G and the resolution of the excess noise.

niobium) on a silicon wafer.[40] A fully assembled SPT-3G wafer module is shown in Figure 3. Each filter network is contained in a single chip and connected to the TES detector wafer using flexible kapton over copper cables and a printed circuit board. The filter chips are connected to the SQUID and bias electronics using superconducting broadside-coupled striplines.[41]

There are two key parameters of the readout system that directly impact total instrument sensitivity: readout yield and readout noise. Crosstalk is also an important systematic effect when evaluating the performance of the fMux readout system. A discussion of crosstalk and the relevant design and features implemented in the SPT-3G readout are found elsewhere.[37,41] Yield will be discussed in Section 4.1 in the context of the total focal plane yield. Here, we focus on the contribution of readout noise to the total noise budget. The noise of the fMux readout system is measured in terms of the noise equivalent current ($NEI_{\rm readout}$) at the bolometer. Transforming this noise level to the readout noise equivalent power requires scaling by the voltage bias ($NEP_{\rm readout} = V_{\rm bias} NEI_{\rm readout}$). Noise is expected from several sources in the fMux system including the signal generation and processing electronics, the resistor used to create the voltage bias, and the intrinsic SQUID noise.[35,42]

During the first year of operation an excess of readout noise was observed in SPT-3G, degrading the instrumental sensitivity compared to expectations. Three improvements were made to the SPT-3G system to resolve this excess. First, a non-optimal instrument grounding scheme was discovered. Noise was entering the highly-sensitive analog ground plane of the SQUID control boards via the shielding braid and foils in the cables that connect to the ADC/DAC mezzanines and field programmable gate array (FPGA) motherboards. These ground connections were disconnected and the readout and instrument noise was dramatically reduced across the entire bandwidth of the electronics. Second, filters on the waveforms output by the carrier and nuller digital-to-analog converters were tightened to better match the actual bandwidth used. This reduced the bandwidth over which external signals could couple to the SQUIDs.

The final source of excess noise in the SPT-3G readout system was a subtle feature of the nulling scheme. DAN injects and actively adjusts a waveform at the input coil of the SQUID to minimize the voltage at this node. However, the current is also able to flow back through the TES/ filter network and bias resistor to ground (see Figure 4). Noise sources introduced into the fMux system after the input coil of the SQUID are measured in the demodulation process and added to the injected nuller. The nuller increases in amplitude to compensate for the current leakage, amplifying the demodulation chain noise in the process. The amount of current that flows through the secondary path is determined by the ratio of impedances between the TES and the SQUID input coil. The effect is therefore proportional to the TES bias frequency, with a negligible contribution at the lowest frequencies but rising to a significant level in the middle of the SPT-3G electronics bandwidth. The typical

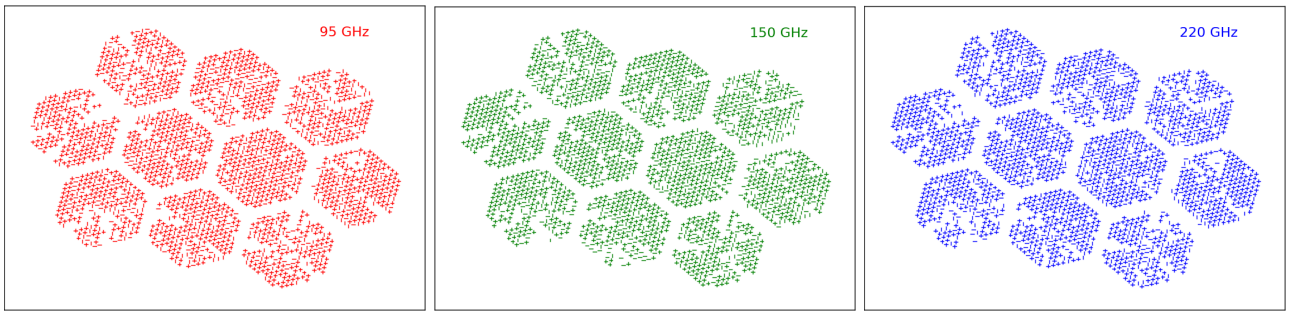

Figure 5. The optically responsive detectors in SPT-3G as a function of their position in the focal plane. Each detector is represented by a line and full polarization pair is shown as a +. The hexagonal shapes of the ten detector wafers are clearly visible. Wedges that are missing from a hexagon represent readout modules in the focal plane that are electrically disconnected. These modules will be repaired during the austral summer of 2018-2019.

operating TES resistance in SPT-3G is roughly $R_{\rm TES} \sim 1.6\,\Omega$. In the first year of operation the SPT-3G fMux used NIST fabricated SQUIDs (SA4 style) with a typical input coil inductance of $L_{\rm SQ} \sim 300$ nH.[38] For the 1.6 - 5.2 MHz bandwidth the SQUID input coil impedance becomes comparable to $R_{\rm TES}$, resulting in significant amplification of the demodulation chain noise. For the second year of operation, new NIST SA13 SQUIDs with a reduced input impedance were installed in the SPT-3G receiver. Additionally, the printed circuit board that the SQUIDs are mounted on was redesigned to remove its contribution to the circuit impedance between the nuller injection point and the SQUID input coil. With a total input coil inductance closer to $L_{\rm SQ} \sim 60 - 80$ nH, less of the nuller current leaks through the TES network and the noise amplification is significantly reduced.

Figure 4 compares the total noise of the SPT-3G detectors currently to the performance before the implementation of the motherboard filtering and low input inductance SQUIDs. For the data in this plot, the detectors were held at a temperature above the superconducting transition. Expected noise sources in this configuration include Johnson noise from the bolometer and the readout noise. The reduction in both the median and scatter in the current noise distribution demonstrates the successful implementation of the improvements discussed here and the mitigation of the excess readout noise.

4. ON-SKY PERFORMANCE

SPT-3G observes several calibration sources as part of its regular cadence for array characterization. These sources include the atmosphere, a chopped blackbody behind the secondary mirror, the galactic HII regions RCW38 and MAT5a, the active galactic nucleus Centaurus A, planets (when available from the South Pole), and quasars. In this section, we present the performance of the SPT-3G receiver in its improved second year configuration based on observations of these calibration sources.

4.1 Array Yield

The leap in sensitivity of the SPT-3G receiver compared to previous CMB experiments is made possible by the large number of TES bolometers. The total number of detectors sensitive to optical signals is therefore critical to achieving the targeted science. Detectors in the array that respond to optical calibration signals are shown in Figure 5. Approximately 11,400 bolometers have optical response and the corresponding losses can be attributed to several different effects. A small fraction of the array is not electrically connected due to an asymmetry in the wiring design of the detector wafer and cryogenic readout. Some detectors fail initial quality control while others do not perform cryogenically. Some yield loss can also be attributed to entire modules that have been disconnected in the cryogenic readout (either a problem with the filter network chip or the stripline connection). These modules are seen in Figure 5 as wedge shaped holes in the hexagonal wafer pattern. Overall, the total yield for typical observations is $\sim 72\%$.[34]

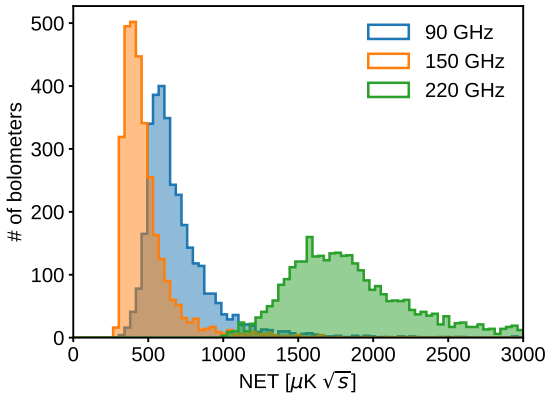

Figure 6. The on-sky distribution of noise equivalent temperatures (NETs) for the SPT-3G receiver. The performance of the 95 and 150 GHz detectors is in reasonable agreement with expectations, however, performance of the 220 GHz detectors is clearly degraded. This effect is thought to be due to poor transmission in the AR coatings on the lenses and is under further investigation.

4.2 Array Noise

Noise equivalent temperature (NET) is used to quantify the sensitivity of the detectors including the noise, bands, and optical efficiency. NET is determined by measuring the noise in the 10 - 15 Hz band during a noise observation taken while the telescope is stationary and calibrating it based on an RCW38 observation. Current analysis suggests that the white noise level in this band is representative of the instrument performance at frequencies of interest. Analysis of the noise at the lowest frequencies (relevant for mapping the largest angular scales on the sky) is ongoing. The distribution of NET for each of the SPT-3G observing bands is shown in Figure 6 and summarized in Table 1. We find median per detector NETs of 630/440/1800 $\mu\mathrm{K}\sqrt{s}$ in the 95/150/220 GHz bands. Given the yield stated above, the total focal plane NET is 10 $\mu\mathrm{K}\sqrt{s}$ at 95 GHz, 8 $\mu\mathrm{K}\sqrt{s}$ at 150 GHz, and 30 $\mu\mathrm{K}\sqrt{s}$ at 220 GHz. The 95 and 150 GHz NETs are reasonably consistent with theoretical predictions for the SPT-3G optical design, however, the 220 GHz NET is about a factor of 1.5 higher than expectations. The non-optimal performance of the 220 GHz detectors is believed to be due to poor transmission in the alumina AR coatings and an investigation is underway to confirm this hypothesis.[43] Despite the performance of the 220 GHz bolometers, the SPT-3G array is significantly more sensitive than SPTpol, with a 9/4 times faster mapping speed at 95/150 GHz.[13,44]

	95 GHz	150 GHz	220 GHz
Beam FWHM (arcmin)	1.6	1.2	1.1
Optically responsive N_{bolo}	3800	3780	3820
$\mathrm{NET}_{\mathrm{bolo},T}$ [$\mu\mathrm{K}\sqrt{s}$]	630	440	1800
$\mathrm{NET}_{\mathrm{array},T}$ [$\mu\mathrm{K}\sqrt{s}$]	10	8	30
Projected Map Depth [μK-arcmin]	3	2	9

Table 1. The measured performance of the SPT-3G receiver as well as projected map depths for the five year 1500 deg^2 survey.

4.3 Survey Strategy

During the first year of SPT-3G commissioning, observations were taken of the SPTpol 500 square degree field. An initial intensity map of these data in the 95 and 150 GHz bands is shown in Figure 7. For its primary science

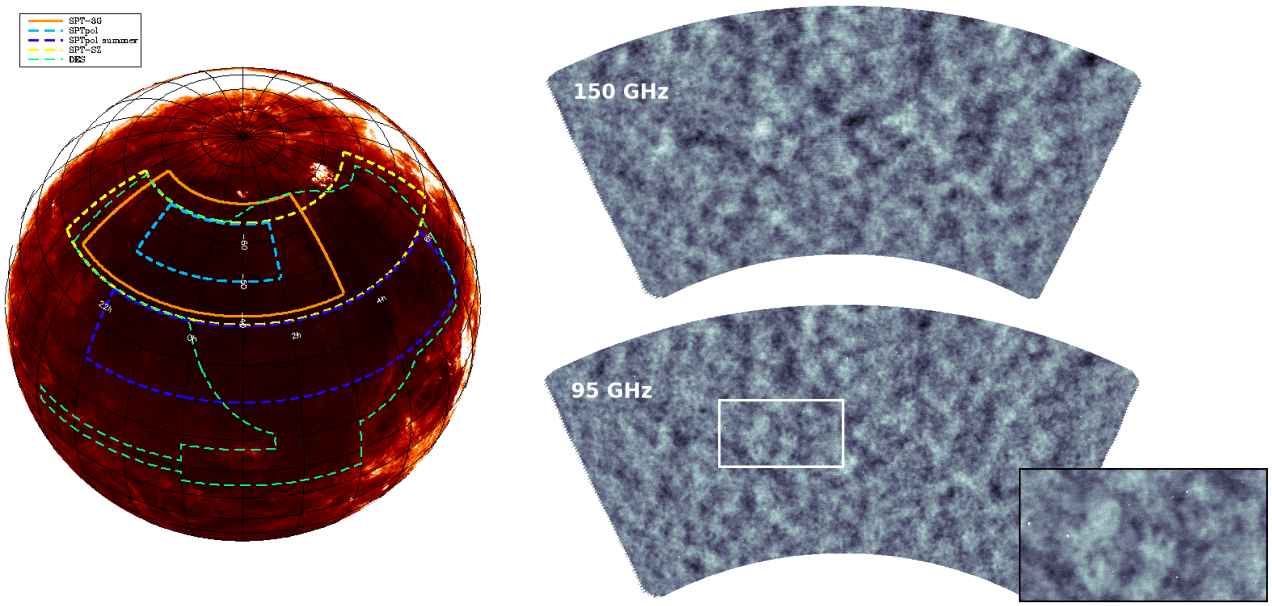

Figure 7. *Left:* The SPT survey fields overlaid on an IRAS dust map of the sky.[47] In this diagram, the south celestial pole is shown pointing up. The main 1500 deg^2 survey field for SPT-3G is shown in orange. The SPTpol 500 deg^2 field was observed during SPT-3G commissioning. The SPT-3G main field is designed for complete coverage of the future BICEP Array field. It also overlaps with existing SPT survey data, with the current BICEP/KECK field (coincident with the SPTpol field),[45] and the DES.[46] *Right:* Intensity maps from SPT-3G commissioning observations of the 500 deg^2 field. Common structure is clearly seen in the larger-scale anisotropies between the two observing bands. Point sources are also visible throughout the map, shown in the 95 GHz inset in the lower right image of the panel.

survey, SPT-3G is observing a 1500 square degree field for a total of five years (from 2018 - 2023). The survey field, shown in Figure 7, overlaps completely with the current BICEP/KECK field as well the future BICEP Array field for joint analyses of the complementary datasets.[45] The SPT-3G survey field also has significant overlap with the Dark Energy Survey (DES) for cross-correlation with optical tracers of LSS.[46] Observations of the 1500 deg^2 field are now ongoing and initial analysis of the data is underway. Given the array sensitivities stated above, final map depths of 3, 2, and 9 μK-arcmin in intensity are expected in the 95, 150, and 220 GHz bands with polarization depths a factor $\sqrt{2}$ higher.

The 1500 deg^2 field is split into two subfields at high and low telescope elevation to prevent dramatic changes in the atmospheric optical loading on the detectors. Observations of each subfield alternate with recycling the millikelvin refrigerator (approximately every 26 hours) and observations of the internal calibrator and galactic HII regions (RCW38 and MAT5a) are interspersed throughout.

5. COSMOLOGICAL FORECASTS

Given the array sensitivity presented in the previous section projections can be made for the intensity (temperature) and polarized CMB power spectra as measured by SPT-3G. Figure 8 shows these projections in comparison with current state-of-the-art datasets. These forecasts highlight how SPT-3G will improve on current constraints, particularly at small angular scales (high multipole moments) on the sky. The damping tail measurements of the E modes will probe both the basic ΛCDM model and the effect of light relics.[16] SPT-3G is expected to constrain the number of light relics with $\sigma(N_{\rm eff}) = 0.1$ through the impact on the expansion rate of the universe at early times seen in the CMB power spectrum damping tail.

The high signal-to-noise measurement of small scale B modes will tightly constrain the gravitational lensing component of the power spectrum. The projection for the SPT-3G measurement of the gravitational lensing power spectrum is shown in Figure 9. From these data, SPT-3G will infer the sum of neutrino mass through its impact on the growth of large scale structure. The expected constraint on the sum of neutrino mass is

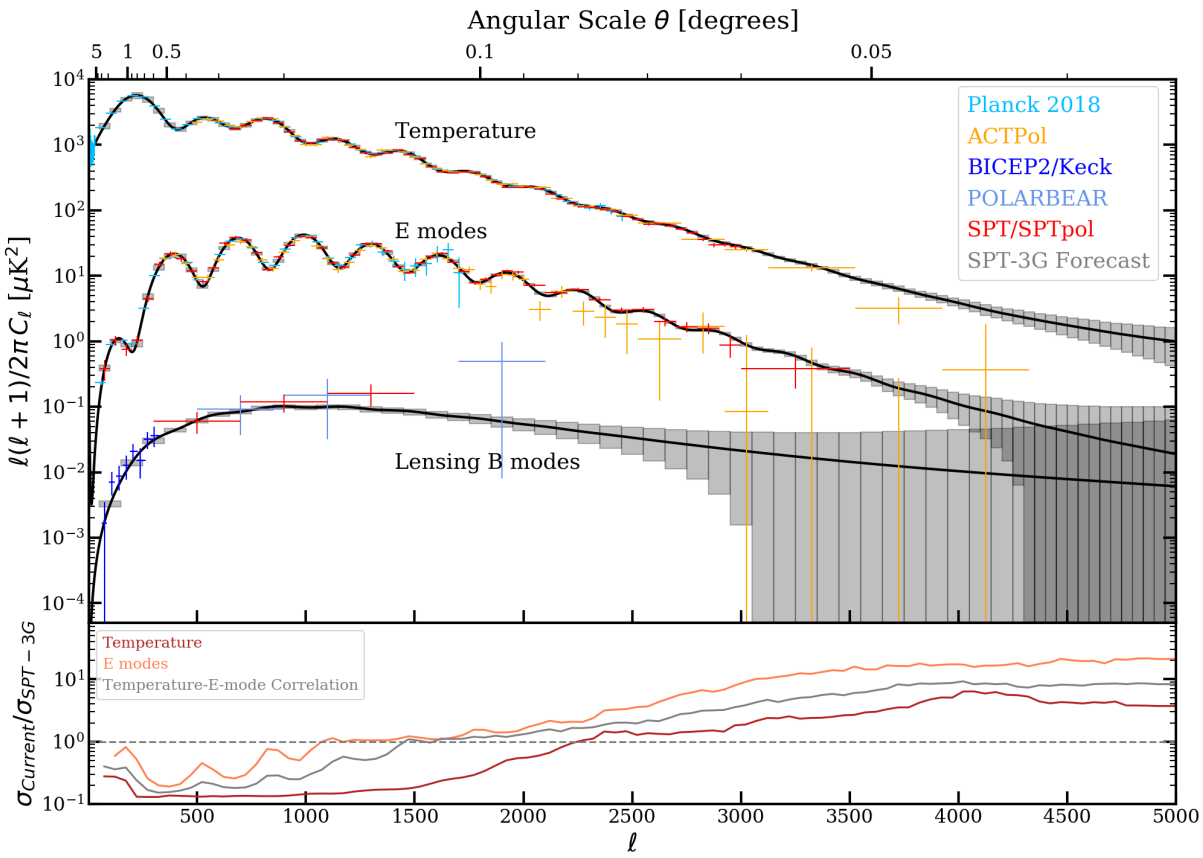

Figure 8. *Top:* Projections for the CMB temperature and polarized power spectra as measured by SPT-3G are depicted by the gray vertical bars. Current state-of-the-art constraints from the *Planck* satellite,[48] BICEP2/KECK,[17] ACTPol,[49] POLARBEAR[50] SPT-SZ,[2] and SPTpol[3,51] experiments are also shown. *Bottom:* Expected improvement in the TT, EE, and TE power spectra for SPT-3G data in comparison to the most sensitive current measurements. SPT-3G will improve on current constraints at the multipoles where these factors are greater than unity (the dashed line).

$\sigma(\Sigma m_\nu) \sim 0.1$ eV, which is approaching an interesting regime for differentiating between possibilities for the neutrino hierarchy.[16] Additionally, the SPT-3G measurement of the lensing B modes will be used to delens large-scale B-mode data in search of inflationary gravitational waves (see Figure 9). As described in Section 4.3 the SPT-3G field fully overlaps with that of the BICEP/KECK survey. SPT-3G will therefore be able to both internally delens its own measurement of the large-scale B modes as well as the data from BICEP/KECK. It is expected that delensing with the SPT-3G data will remove approximately 2/3 of the lensing power, tightening constraints on inflationary B modes.

6. SUMMARY

The SPT-3G receiver is a high throughput, broadband (95/150/220 GHz), polarization-sensitive TES bolometer camera designed for high resolution observations of the CMB. We presented here the status and performance of SPT-3G in its second year of operations. Based on the initial year of commissioning and calibration observations in 2017, several improvements were made to the receiver for the 2018 observing season. A new PTFE based anti-reflection coating technology was used to apply three-layer coatings to the large cryogenic alumina lenses. New detectors with optimized saturation power were fabricated and installed. Lastly, excess noise in the readout system was successfully mitigated by improving grounding and installing lower input impedance SQUIDs. With these improvements all three bands show performance consistent with photon-noise domination. The 220 GHz band shows some degradation of sensitivity and an investigation of the optical throughput is underway. There

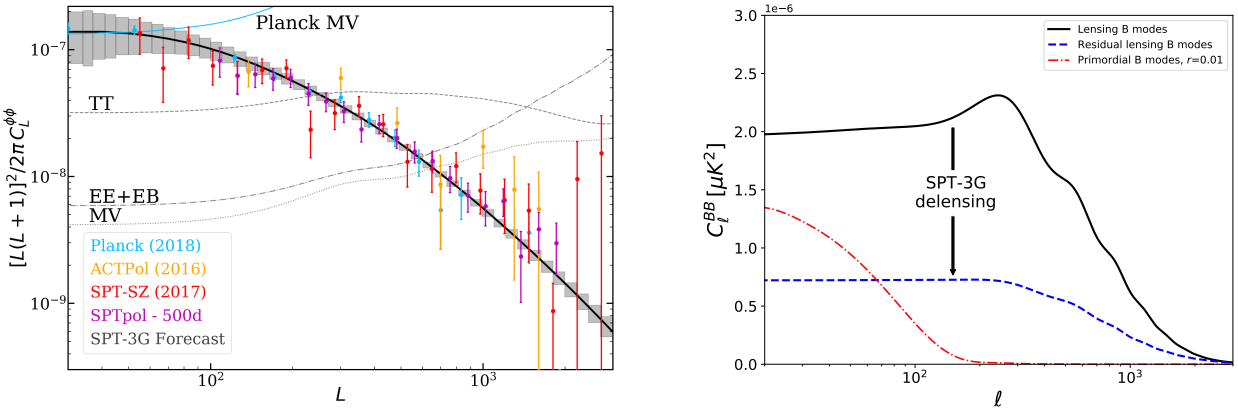

Figure 9. *Left:* Projected SPT-3G measurement of the CMB gravitational lensing power spectrum, along with current measurements from the *Planck* satellite,[52] SPT-SZ,[4] SPTpol,[5,6] and ACTPol.[53] Noise curves are shown for different combinations of the lensing estimator (TT only, EE + EB, and the minimum variance combination of all temperature and polarization estimators). For lensing modes smaller than the mode at which the two curves cross, SPT-3G will have signal-to-noise greater than unity on individual sky features. *Right:* The projected cleaning of the gravitational lensing signal from the B-mode power spectrum using the SPT-3G data (black and blue dashed). For comparison, a primordial B-mode spectrum due to inflationary gravitational waves is shown.

are approximately 11,400 optically responsive TES bolometers in the full focal plane, making the SPT-3G camera one of the most sensitive CMB cameras currently observing. SPT-3G has now begun a five year survey of its primary 1500 deg^2 field. The exceptional sensitivity of the resulting CMB E- and B-mode polarization maps will lead to a wide variety of millimeter-wavelength point source astrophysics, tight constraints on neutrino mass, and delensing of the B-mode signal for inflationary studies.

7. ACKNOWLEDGEMENTS

The South Pole Telescope program is supported by the National Science Foundation (NSF) through grant PLR-1248097. Partial support is also provided by the NSF Physics Frontier Center grant PHY-1125897 to the Kavli Institute of Cosmological Physics at the University of Chicago, the Kavli Foundation, and the Gordon and Betty Moore Foundation through grant GBMF#947 to the University of Chicago. Work at Argonne National Lab is supported by UChicago Argonne LLC, Operator of Argonne National Laboratory (Argonne). Argonne, a U.S. Department of Energy Office of Science Laboratory, is operated under contract no. DE-AC02-06CH11357. We acknowledge R. Divan, L. Stan, C.S. Miller, and V. Kutepova for supporting our work in the Argonne Center for Nanoscale Materials. Work at Fermi National Accelerator Laboratory, a DOE-OS, HEP User Facility managed by the Fermi Research Alliance, LLC, was supported under Contract No. DE-AC02-07CH11359. NWH acknowledges support from NSF CAREER grant AST-0956135. The McGill authors acknowledge funding from the Natural Sciences and Engineering Research Council of Canada, Canadian Institute for Advanced Research, and the Fonds de recherche du Qubec Nature et technologies. CR acknowledges support from the Australian Research Councils Future Fellowships scheme (FT150100074). JV acknowledges support from the Sloan Foundation.

REFERENCES

[1] Carlstrom, J. E., Ade, P. A. R., Aird, K. A., Benson, B. A., Bleem, L. E., Busetti, S., Chang, C. L., Chauvin, E., Cho, H.-M., Crawford, T. M., Crites, A. T., Dobbs, M. A., Halverson, N. W., Heimsath, S., Holzapfel, W. L., Hrubes, J. D., Joy, M., Keisler, R., Lanting, T. M., Lee, A. T., Leitch, E. M., Leong, J., Lu, W., Lueker, M., Luong-Van, D., McMahon, J. J., Mehl, J., Meyer, S. S., Mohr, J. J., Montroy, T. E., Padin, S., Plagge, T., Pryke, C., Ruhl, J. E., Schaffer, K. K., Schwan, D., Shirokoff, E., Spieler, H. G., Staniszewski,

Z., Stark, A. A., Tucker, C., Vanderlinde, K., Vieira, J. D., and Williamson, R., "The 10 Meter South Pole Telescope," *PASP* **123**, 568–581 (May 2011).

[2] Story, K. T., Reichardt, C. L., Hou, Z., Keisler, R., Aird, K. A., Benson, B. A., Bleem, L. E., Carlstrom, J. E., Chang, C. L., Cho, H.-M., Crawford, T. M., Crites, A. T., de Haan, T., Dobbs, M. A., Dudley, J., Follin, B., George, E. M., Halverson, N. W., Holder, G. P., Holzapfel, W. L., Hoover, S., Hrubes, J. D., Joy, M., Knox, L., Lee, A. T., Leitch, E. M., Lueker, M., Luong-Van, D., McMahon, J. J., Mehl, J., Meyer, S. S., Millea, M., Mohr, J. J., Montroy, T. E., Padin, S., Plagge, T., Pryke, C., Ruhl, J. E., Sayre, J. T., Schaffer, K. K., Shaw, L., Shirokoff, E., Spieler, H. G., Staniszewski, Z., Stark, A. A., van Engelen, A., Vanderlinde, K., Vieira, J. D., Williamson, R., and Zahn, O., "A Measurement of the Cosmic Microwave Background Damping Tail from the 2500-Square-Degree SPT-SZ Survey," *ApJ* **779**, 86 (Dec. 2013).

[3] Henning, J. W., Sayre, J. T., Reichardt, C. L., Ade, P. A. R., Anderson, A. J., Austermann, J. E., Beall, J. A., Bender, A. N., Benson, B. A., Bleem, L. E., Carlstrom, J. E., Chang, C. L., Chiang, H. C., Cho, H.-M., Citron, R., Corbett Moran, C., Crawford, T. M., Crites, A. T., de Haan, T., Dobbs, M. A., Everett, W., Gallicchio, J., George, E. M., Gilbert, A., Halverson, N. W., Harrington, N., Hilton, G. C., Holder, G. P., Holzapfel, W. L., Hoover, S., Hou, Z., Hrubes, J. D., Huang, N., Hubmayr, J., Irwin, K. D., Keisler, R., Knox, L., Lee, A. T., Leitch, E. M., Li, D., Lowitz, A., Manzotti, A., McMahon, J. J., Meyer, S. S., Mocanu, L., Montgomery, J., Nadolski, A., Natoli, T., Nibarger, J. P., Novosad, V., Padin, S., Pryke, C., Ruhl, J. E., Saliwanchik, B. R., Schaffer, K. K., Sievers, C., Smecher, G., Stark, A. A., Story, K. T., Tucker, C., Vanderlinde, K., Veach, T., Vieira, J. D., Wang, G., Whitehorn, N., Wu, W. L. K., and Yefremenko, V., "Measurements of the Temperature and E-mode Polarization of the CMB from 500 Square Degrees of SPTpol Data," *ApJ* **852**, 97 (Jan. 2018).

[4] Omori, Y., Chown, R., Simard, G., Story, K. T., Aylor, K., Baxter, E. J., Benson, B. A., Bleem, L. E., Carlstrom, J. E., Chang, C. L., Cho, H.-M., Crawford, T. M., Crites, A. T., de Haan, T., Dobbs, M. A., Everett, W. B., George, E. M., Halverson, N. W., Harrington, N. L., Holder, G. P., Hou, Z., Holzapfel, W. L., Hrubes, J. D., Knox, L., Lee, A. T., Leitch, E. M., Luong-Van, D., Manzotti, A., Marrone, D. P., McMahon, J. J., Meyer, S. S., Mocanu, L. M., Mohr, J. J., Natoli, T., Padin, S., Pryke, C., Reichardt, C. L., Ruhl, J. E., Sayre, J. T., Schaffer, K. K., Shirokoff, E., Staniszewski, Z., Stark, A. A., Vanderlinde, K., Vieira, J. D., Williamson, R., and Zahn, O., "A 2500 deg^2 CMB Lensing Map from Combined South Pole Telescope and Planck Data," *ApJ* **849**, 124 (Nov. 2017).

[5] Story, K. T., Hanson, D., Ade, P. A. R., Aird, K. A., Austermann, J. E., Beall, J. A., Bender, A. N., Benson, B. A., Bleem, L. E., Carlstrom, J. E., Chang, C. L., Chiang, H. C., Cho, H.-M., Citron, R., Crawford, T. M., Crites, A. T., de Haan, T., Dobbs, M. A., Everett, W., Gallicchio, J., Gao, J., George, E. M., Gilbert, A., Halverson, N. W., Harrington, N., Henning, J. W., Hilton, G. C., Holder, G. P., Holzapfel, W. L., Hoover, S., Hou, Z., Hrubes, J. D., Huang, N., Hubmayr, J., Irwin, K. D., Keisler, R., Knox, L., Lee, A. T., Leitch, E. M., Li, D., Liang, C., Luong-Van, D., McMahon, J. J., Mehl, J., Meyer, S. S., Mocanu, L., Montroy, T. E., Natoli, T., Nibarger, J. P., Novosad, V., Padin, S., Pryke, C., Reichardt, C. L., Ruhl, J. E., Saliwanchik, B. R., Sayre, J. T., Schaffer, K. K., Smecher, G., Stark, A. A., Tucker, C., Vanderlinde, K., Vieira, J. D., Wang, G., Whitehorn, N., Yefremenko, V., and Zahn, O., "A Measurement of the Cosmic Microwave Background Gravitational Lensing Potential from 100 Square Degrees of SPTpol Data," *ApJ* **810**, 50 (Sept. 2015).

[6] Mocanu, M. and et al. *in preparation* (2018).

[7] Bleem, L. E., Stalder, B., de Haan, T., Aird, K. A., Allen, S. W., Applegate, D. E., Ashby, M. L. N., Bautz, M., Bayliss, M., Benson, B. A., Bocquet, S., Brodwin, M., Carlstrom, J. E., Chang, C. L., Chiu, I., Cho, H. M., Clocchiatti, A., Crawford, T. M., Crites, A. T., Desai, S., Dietrich, J. P., Dobbs, M. A., Foley, R. J., Forman, W. R., George, E. M., Gladders, M. D., Gonzalez, A. H., Halverson, N. W., Hennig, C., Hoekstra, H., Holder, G. P., Holzapfel, W. L., Hrubes, J. D., Jones, C., Keisler, R., Knox, L., Lee, A. T., Leitch, E. M., Liu, J., Lueker, M., Luong-Van, D., Mantz, A., Marrone, D. P., McDonald, M., McMahon, J. J., Meyer, S. S., Mocanu, L., Mohr, J. J., Murray, S. S., Padin, S., Pryke, C., Reichardt, C. L., Rest, A., Ruel, J., Ruhl, J. E., Saliwanchik, B. R., Saro, A., Sayre, J. T., Schaffer, K. K., Schrabback, T., Shirokoff, E., Song, J., Spieler, H. G., Stanford, S. A., Staniszewski, Z., Stark, A. A., Story, K. T., Stubbs, C. W., Vanderlinde, K., Vieira, J. D., Vikhlinin, A., Williamson, R., Zahn, O., and Zenteno, A., "Galaxy Clusters Discovered via the Sunyaev-Zel'dovich Effect in the 2500-Square-Degree SPT-SZ Survey," *ApJS* **216**, 27 (Feb. 2015).

[8] de Haan, T., Benson, B. A., Bleem, L. E., Allen, S. W., Applegate, D. E., Ashby, M. L. N., Bautz, M., Bayliss, M., Bocquet, S., Brodwin, M., Carlstrom, J. E., Chang, C. L., Chiu, I., Cho, H.-M., Clocchiatti, A., Crawford, T. M., Crites, A. T., Desai, S., Dietrich, J. P., Dobbs, M. A., Doucouliagos, A. N., Foley, R. J., Forman, W. R., Garmire, G. P., George, E. M., Gladders, M. D., Gonzalez, A. H., Gupta, N., Halverson, N. W., Hlavacek-Larrondo, J., Hoekstra, H., Holder, G. P., Holzapfel, W. L., Hou, Z., Hrubes, J. D., Huang, N., Jones, C., Keisler, R., Knox, L., Lee, A. T., Leitch, E. M., von der Linden, A., Luong-Van, D., Mantz, A., Marrone, D. P., McDonald, M., McMahon, J. J., Meyer, S. S., Mocanu, L. M., Mohr, J. J., Murray, S. S., Padin, S., Pryke, C., Rapetti, D., Reichardt, C. L., Rest, A., Ruel, J., Ruhl, J. E., Saliwanchik, B. R., Saro, A., Sayre, J. T., Schaffer, K. K., Schrabback, T., Shirokoff, E., Song, J., Spieler, H. G., Stalder, B., Stanford, S. A., Staniszewski, Z., Stark, A. A., Story, K. T., Stubbs, C. W., Vanderlinde, K., Vieira, J. D., Vikhlinin, A., Williamson, R., and Zenteno, A., "Cosmological Constraints from Galaxy Clusters in the 2500 Square-degree SPT-SZ Survey," *ApJ* **832**, 95 (Nov. 2016).

[9] Whitehorn, N., Natoli, T., Ade, P. A. R., Austermann, J. E., Beall, J. A., Bender, A. N., Benson, B. A., Bleem, L. E., Carlstrom, J. E., Chang, C. L., Chiang, H. C., Cho, H.-M., Citron, R., Crawford, T. M., Crites, A. T., de Haan, T., Dobbs, M. A., Everett, W., Gallicchio, J., George, E. M., Gilbert, A., Halverson, N. W., Harrington, N., Henning, J. W., Hilton, G. C., Holder, G. P., Holzapfel, W. L., Hoover, S., Hou, Z., Hrubes, J. D., Huang, N., Hubmayr, J., Irwin, K. D., Keisler, R., Knox, L., Lee, A. T., Leitch, E. M., Li, D., McMahon, J. J., Meyer, S. S., Mocanu, L., Nibarger, J. P., Novosad, V., Padin, S., Pryke, C., Reichardt, C. L., Ruhl, J. E., Saliwanchik, B. R., Sayre, J. T., Schaffer, K. K., Smecher, G., Stark, A. A., Story, K. T., Tucker, C., Vanderlinde, K., Vieira, J. D., Wang, G., and Yefremenko, V., "Millimeter Transient Point Sources in the SPTpol 100 Square Degree Survey," *ApJ* **830**, 143 (Oct. 2016).

[10] Anderson, A. J., Ade, P. A. R., Ahmed, Z., Austermann, J. E., Avva, J. S., Barry, P. S., Thakur, R. B., Bender, A. N., Benson, B. A., Bleem, L. E., Byrum, K., Carlstrom, J. E., Carter, F. W., Cecil, T., Chang, C. L., Cho, H. M., Cliche, J. F., Crawford, T. M., Cukierman, A., Denison, E. V., de Haan, T., Ding, J., Dobbs, M. A., Dutcher, D., Everett, W., Foster, A., Gannon, R. N., Gilbert, A., Groh, J. C., Halverson, N. W., Harke-Hosemann, A. H., Harrington, N. L., Henning, J. W., Hilton, G. C., Holder, G. P., Holzapfel, W. L., Huang, N., Irwin, K. D., Jeong, O. B., Jonas, M., Khaire, T., Knox, L., Kofman, A. M., Korman, M., Kubik, D., Kuhlmann, S., Kuklev, N., Kuo, C. L., Lee, A. T., Leitch, E. M., Lowitz, A. E., Meyer, S. S., Michalik, D., Montgomery, J., Nadolski, A., Natoli, T., Nguyen, H., Noble, G. I., Novosad, V., Padin, S., Pan, Z., Pearson, J., Posada, C. M., Rahlin, A., Reichardt, C. L., Ruhl, J. E., Saunders, L. J., Sayre, J. T., Shirley, I., Shirokoff, E., Smecher, G., Sobrin, J. A., Stark, A. A., Story, K. T., Suzuki, A., Tang, Q. Y., Thompson, K. L., Tucker, C., Vale, L. R., Vanderlinde, K., Vieira, J. D., Wang, G., Whitehorn, N., Yefremenko, V., Yoon, K. W., and Young, M. R., "Spt-3g: A multichroic receiver for the south pole telescope," *Journal of Low Temperature Physics* (Jul 2018).

[11] Pan, Z., Ade, P. A. R., Ahmed, Z., Anderson, A. J., Austermann, J. E., Avva, J. S., Thakur, R. B., Bender, A. N., Benson, B. A., Carlstrom, J. E., Carter, F. W., Cecil, T., Chang, C. L., Cliche, J. F., Cukierman, A., Denison, E. V., de Haan, T., Ding, J., Dobbs, M. A., Dutcher, D., Everett, W., Foster, A., Gannon, R. N., Gilbert, A., Groh, J. C., Halverson, N. W., Harke-Hosemann, A. H., Harrington, N. L., Henning, J. W., Hilton, G. C., Holzapfel, W. L., Huang, N., Irwin, K. D., Jeong, O. B., Jonas, M., Khaire, T., Kofman, A. M., Korman, M., Kubik, D., Kuhlmann, S., Kuo, C. L., Lee, A. T., Lowitz, A. E., Meyer, S. S., Michalik, D., Montgomery, J., Nadolski, A., Natoli, T., Nguyen, H., Noble, G. I., Novosad, V., Padin, S., Pearson, J., Posada, C. M., Rahlin, A., Ruhl, J. E., Saunders, L. J., Sayre, J. T., Shirley, I., Shirokoff, E., Smecher, G., Sobrin, J. A., Stark, A. A., Story, K. T., Suzuki, A., Tang, Q. Y., Thompson, K. L., Tucker, C., Vale, L. R., Vanderlinde, K., Vieira, J. D., Wang, G., Whitehorn, N., Yefremenko, V., Yoon, K. W., and Young, M. R., "Optical Characterization of the SPT-3G Camera," *Journal of Low Temperature Physics* (May 2018).

[12] Everett, W. and et al, "Design and bolometer characterization of the spt-3g first-year focal plane," *submitted to Journal of Low Temperature Physics* (2018).

[13] Benson, B. A., Ade, P. A. R., Ahmed, Z., Allen, S. W., Arnold, K., Austermann, J. E., Bender, A. N., Bleem, L. E., Carlstrom, J. E., Chang, C. L., Cho, H. M., Cliche, J. F., Crawford, T. M., Cukierman, A., de Haan, T., Dobbs, M. A., Dutcher, D., Everett, W., Gilbert, A., Halverson, N. W., Hanson, D., Harrington, N. L., Hattori, K., Henning, J. W., Hilton, G. C., Holder, G. P., Holzapfel, W. L., Irwin, K. D., Keisler, R., Knox, L., Kubik, D., Kuo, C. L., Lee, A. T., Leitch, E. M., Li, D., McDonald, M., Meyer, S. S., Montgomery, J.,

Myers, M., Natoli, T., Nguyen, H., Novosad, V., Padin, S., Pan, Z., Pearson, J., Reichardt, C., Ruhl, J. E., Saliwanchik, B. R., Simard, G., Smecher, G., Sayre, J. T., Shirokoff, E., Stark, A. A., Story, K., Suzuki, A., Thompson, K. L., Tucker, C., Vanderlinde, K., Vieira, J. D., Vikhlinin, A., Wang, G., Yefremenko, V., and Yoon, K. W., "SPT-3G: a next-generation cosmic microwave background polarization experiment on the South Pole telescope," in [*Millimeter, Submillimeter, and Far-Infrared Detectors and Instrumentation for Astronomy VII*], *Proc. SPIE* **9153**, 91531P (July 2014).

[14] Hu, W. and Dodelson, S., "Cosmic Microwave Background Anisotropies," *ARA&A* **40**, 171–216 (2002).

[15] Freedman, W. L., "Correction: Cosmology at a crossroads," *Nature Astronomy* **1**, 0169 (June 2017).

[16] Abazajian, K. N., Adshead, P., Ahmed, Z., Allen, S. W., Alonso, D., Arnold, K. S., Baccigalupi, C., Bartlett, J. G., Battaglia, N., Benson, B. A., Bischoff, C. A., Borrill, J., Buza, V., Calabrese, E., Caldwell, R., Carlstrom, J. E., Chang, C. L., Crawford, T. M., Cyr-Racine, F.-Y., De Bernardis, F., de Haan, T., di Serego Alighieri, S., Dunkley, J., Dvorkin, C., Errard, J., Fabbian, G., Feeney, S., Ferraro, S., Filippini, J. P., Flauger, R., Fuller, G. M., Gluscevic, V., Green, D., Grin, D., Grohs, E., Henning, J. W., Hill, J. C., Hlozek, R., Holder, G., Holzapfel, W., Hu, W., Huffenberger, K. M., Keskitalo, R., Knox, L., Kosowsky, A., Kovac, J., Kovetz, E. D., Kuo, C.-L., Kusaka, A., Le Jeune, M., Lee, A. T., Lilley, M., Loverde, M., Madhavacheril, M. S., Mantz, A., Marsh, D. J. E., McMahon, J., Meerburg, P. D., Meyers, J., Miller, A. D., Munoz, J. B., Nguyen, H. N., Niemack, M. D., Peloso, M., Peloton, J., Pogosian, L., Pryke, C., Raveri, M., Reichardt, C. L., Rocha, G., Rotti, A., Schaan, E., Schmittfull, M. M., Scott, D., Sehgal, N., Shandera, S., Sherwin, B. D., Smith, T. L., Sorbo, L., Starkman, G. D., Story, K. T., van Engelen, A., Vieira, J. D., Watson, S., Whitehorn, N., and Kimmy Wu, W. L., [*CMB-S4 Science Book, First Edition*], ArXiv1610.02743 (Oct. 2016).

[17] BICEP2 Collaboration, Keck Array Collaboration, Ade, P. A. R., Ahmed, Z., Aikin, R. W., Alexander, K. D., Barkats, D., Benton, S. J., Bischoff, C. A., Bock, J. J., Bowens-Rubin, R., Brevik, J. A., Buder, I., Bullock, E., Buza, V., Connors, J., Crill, B. P., Duband, L., Dvorkin, C., Filippini, J. P., Fliescher, S., Grayson, J., Halpern, M., Harrison, S., Hilton, G. C., Hui, H., Irwin, K. D., Karkare, K. S., Karpel, E., Kaufman, J. P., Keating, B. G., Kefeli, S., Kernasovskiy, S. A., Kovac, J. M., Kuo, C. L., Leitch, E. M., Lueker, M., Megerian, K. G., Netterfield, C. B., Nguyen, H. T., O'Brient, R., Ogburn, R. W., Orlando, A., Pryke, C., Richter, S., Schwarz, R., Sheehy, C. D., Staniszewski, Z. K., Steinbach, B., Sudiwala, R. V., Teply, G. P., Thompson, K. L., Tolan, J. E., Tucker, C., Turner, A. D., Vieregg, A. G., Weber, A. C., Wiebe, D. V., Willmert, J., Wong, C. L., Wu, W. L. K., and Yoon, K. W., "Improved Constraints on Cosmology and Foregrounds from BICEP2 and Keck Array Cosmic Microwave Background Data with Inclusion of 95 GHz Band," *Physical Review Letters* **116**, 031302 (Jan. 2016).

[18] BICEP2/Keck Collaboration, Planck Collaboration, Ade, P. A. R., Aghanim, N., Ahmed, Z., Aikin, R. W., Alexander, K. D., Arnaud, M., Aumont, J., Baccigalupi, C., and et al., "Joint Analysis of BICEP2/Keck Array and Planck Data," *Physical Review Letters* **114**, 101301 (Mar. 2015).

[19] Planck Collaboration, Akrami, Y., Ashdown, M., Aumont, J., Baccigalupi, C., Ballardini, M., Banday, A. J., Barreiro, R. B., Bartolo, N., Basak, S., Benabed, K., Bersanelli, M., Bielewicz, P., Bond, J. R., Borrill, J., Bouchet, F. R., Boulanger, F., Bucher, M., Burigana, C., Calabrese, E., Cardoso, J.-F., Carron, J., Casaponsa, B., Challinor, A., Colombo, L. P. L., Combet, C., Crill, B. P., Cuttaia, F., de Bernardis, P., de Rosa, A., de Zotti, G., Delabrouille, J., Delouis, J.-M., Di Valentino, E., Dickinson, C., Diego, J. M., Donzelli, S., Doré, O., Ducout, A., Dupac, X., Efstathiou, G., Elsner, F., Enßlin, T. A., Eriksen, H. K., Falgarone, E., Fernandez-Cobos, R., Finelli, F., Forastieri, F., Frailis, M., Fraisse, A. A., Franceschi, E., Frolov, A., Galeotta, S., Galli, S., Ganga, K., Génova-Santos, R. T., Gerbino, M., Ghosh, T., González-Nuevo, J., Górski, K. M., Gratton, S., Gruppuso, A., Gudmundsson, J. E., Handley, W., Hansen, F. K., Helou, G., Herranz, D., Huang, Z., Jaffe, A. H., Karakci, A., Keihänen, E., Keskitalo, R., Kiiveri, K., Kim, J., Kisner, T. S., Krachmalnicoff, N., Kunz, M., Kurki-Suonio, H., Lagache, G., Lamarre, J.-M., Lasenby, A., Lattanzi, M., Lawrence, C. R., Le Jeune, M., Levrier, F., Liguori, M., Lilje, P. B., Lindholm, V., López-Caniego, M., Lubin, P. M., Ma, Y.-Z., Macías-Pérez, J. F., Maggio, G., Maino, D., Mandolesi, N., Mangilli, A., Marcos-Caballero, A., Martin, P. G., Martínez-González, E., Matarrese, S., Mauri, N., McEwen, J. D., Meinhold, P. R., Melchiorri, A., Mennella, A., Migliaccio, M., Miville-Deschênes, M.-A., Molinari, D., Moneti, A., Montier, L., Morgante, G., Natoli, P., Oppizzi, F., Pagano, L., Paoletti, D., Partridge, B., Peel, M., Pettorino, V., Piacentini, F., Polenta, G., Puget, J.-L., Rachen, J. P., Reinecke,

M., Remazeilles, M., Renzi, A., Rocha, G., Roudier, G., Rubiño-Martín, J. A., Ruiz-Granados, B., Salvati, L., Sandri, M., Savelainen, M., Scott, D., Seljebotn, D. S., Sirignano, C., Spencer, L. D., Suur-Uski, A.-S., Tauber, J. A., Tavagnacco, D., Tenti, M., Thommesen, H., Toffolatti, L., Tomasi, M., Trombetti, T., Valiviita, J., Van Tent, B., Vielva, P., Villa, F., Vittorio, N., Wandelt, B. D., Wehus, I. K., Zacchei, A., and Zonca, A., "Planck 2018 results. IV. Diffuse component separation," *ArXiv e-prints* (July 2018).

[20] Carron, J., Lewis, A., and Challinor, A., "Internal delensing of Planck CMB temperature and polarization," *J. Cosmology Astropart. Phys.* **5**, 035 (May 2017).

[21] Manzotti, A., Story, K. T., Wu, W. L. K., Austermann, J. E., Beall, J. A., Bender, A. N., Benson, B. A., Bleem, L. E., Bock, J. J., Carlstrom, J. E., Chang, C. L., Chiang, H. C., Cho, H.-M., Citron, R., Conley, A., Crawford, T. M., Crites, A. T., de Haan, T., Dobbs, M. A., Dodelson, S., Everett, W., Gallicchio, J., George, E. M., Gilbert, A., Halverson, N. W., Harrington, N., Henning, J. W., Hilton, G. C., Holder, G. P., Holzapfel, W. L., Hoover, S., Hou, Z., Hrubes, J. D., Huang, N., Hubmayr, J., Irwin, K. D., Keisler, R., Knox, L., Lee, A. T., Leitch, E. M., Li, D., McMahon, J. J., Meyer, S. S., Mocanu, L. M., Natoli, T., Nibarger, J. P., Novosad, V., Padin, S., Pryke, C., Reichardt, C. L., Ruhl, J. E., Saliwanchik, B. R., Sayre, J. T., Schaffer, K. K., Smecher, G., Stark, A. A., Vanderlinde, K., Vieira, J. D., Viero, M. P., Wang, G., Whitehorn, N., Yefremenko, V., and Zemcov, M., "CMB Polarization B-mode Delensing with SPTpol and Herschel," *ApJ* **846**, 45 (Sept. 2017).

[22] Sunyaev, R. A. and Zel'dovich, Y. B., "The observations of relic radiation as a test of the nature of x-ray radiation from the clusters of galaxies," *Comments on Astrophysics* **4**, 173–178 (1972).

[23] Carlstrom, J. E., Holder, G., and Reese, E. D., "Cosmology with the sunyaev-zel'dovich effect," *ARA&A* **40**, 643–680 (2002).

[24] Vieira, J. D., Crawford, T. M., Switzer, E. R., Ade, P. A. R., Aird, K. A., Ashby, M. L. N., Benson, B. A., Bleem, L. E., Brodwin, M., Carlstrom, J. E., Chang, C. L., Cho, H.-M., Crites, A. T., de Haan, T., Dobbs, M. A., Everett, W., George, E. M., Gladders, M., Hall, N. R., Halverson, N. W., High, F. W., Holder, G. P., Holzapfel, W. L., Hrubes, J. D., Joy, M., Keisler, R., Knox, L., Lee, A. T., Leitch, E. M., Lueker, M., Marrone, D. P., McIntyre, V., McMahon, J. J., Mehl, J., Meyer, S. S., Mohr, J. J., Montroy, T. E., Padin, S., Plagge, T., Pryke, C., Reichardt, C. L., Ruhl, J. E., Schaffer, K. K., Shaw, L., Shirokoff, E., Spieler, H. G., Stalder, B., Staniszewski, Z., Stark, A. A., Vanderlinde, K., Walsh, W., Williamson, R., Yang, Y., Zahn, O., and Zenteno, A., "Extragalactic Millimeter-wave Sources in South Pole Telescope Survey Data: Source Counts, Catalog, and Statistics for an 87 Square-degree Field," *ApJ* **719**, 763–783 (Aug. 2010).

[25] Nadolski, A., Kofman, A. M., Vieira, J. D., Ade, P. A. R., Ahmed, Z., Anderson, A. J., Avva, J. S., Basu Thakur, R., Bender, A. N., Benson, B. A., Carlstrom, J. E., Carter, F. W., Cecil, T. W., Chang, C. L., Cliche, J. F., Cukierman, A., de Haan, T., Ding, J., Dobbs, M. A., Dutcher, D., Everett, W., Foster, A., Fu, J., Gallichio, J., Gilbert, A., Groh, J. C., Guns, S. T., Guyser, R., Halverson, N. W., Harke-Hosemann, A. H., Harrington, N. L., Henning, J. W., Holzapfel, W. L., Huang, N., Irwin, K. D., Jeong, O. B., Jonas, M., Jones, A., Khaire, T. S., Korman, M., Kubik, D. L., Kuhlmann, S., Kuo, C.-L., Lee, A. T., Lowitz, A. E., Meyer, S. S., Michalik, D., Montgomery, J., Natoli, T., Nguyen, H., Noble, G. I., Novosad, V., Padin, S., Pan, Z., Pearson, J., Posada, C. M., Quan, W., Rahlin, A., Ruhl, J. E., Sayre, J. T., Shirokoff, E., Smecher, G., Sobrin, J. A., Stark, A. A., Story, K. T., Suzuki, A., Thompson, K. L., Tucker, C., Vanderlinde, K., Wang, G., Whitehorn, N., Yefremenko, V., Yoon, K. W., and Young, M. R., "Broadband anti-reflective coatings for cosmic microwave background experiments," *Proc.SPIE* **10708**, 10708 – 10708 – 13 (2018).

[26] Raguin, D. H. and Morris, G. M., "Analysis of antireflection-structured surfaces with continuous one-dimensional surface profiles," *Appl. Opt.* **32**, 2582–2598 (May 1993).

[27] Jeong, O., Lee, A., Raum, C., and Suzuki, A., "Broadband Plasma-Sprayed Anti-reflection Coating for Millimeter-Wave Astrophysics Experiments," *Journal of Low Temperature Physics* **184**, 621–626 (Aug. 2016).

[28] O'Brient, R., Ade, P., Arnold, K., Edwards, J., Engargiola, G., Holzapfel, W. L., Lee, A. T., Myers, M. J., Quealy, E., Rebeiz, G., Richards, P., and Suzuki, A., "A dual-polarized broadband planar antenna and channelizing filter bank for millimeter wavelengths," *Applied Physics Letters* **102**, 063506 (Feb. 2013).

[29] Carter, F. W., Ade, P. A. R., Ahmed, Z., Anderson, A. J., Austermann, J. E., Avva, J. S., Thakur, R. B., Bender, A. N., Benson, B. A., Carlstrom, J. E., Cecil, T., Chang, C. L., Cliche, J. F., Cukierman, A., Denison, E. V., de Haan, T., Ding, J., Divan, R., Dobbs, M. A., Dutcher, D., Everett, W., Foster, A., Gannon, R. N., Gilbert, A., Groh, J. C., Halverson, N. W., Harke-Hosemann, A. H., Harrington, N. L., Henning, J. W., Hilton, G. C., Holzapfel, W. L., Huang, N., Irwin, K. D., Jeong, O. B., Jonas, M., Khaire, T., Kofman, A. M., Korman, M., Kubik, D., Kuhlmann, S., Kuo, C. L., Kutepova, V., Lee, A. T., Lowitz, A. E., Meyer, S. S., Michalik, D., Miller, C. S., Montgomery, J., Nadolski, A., Natoli, T., Nguyen, H., Noble, G. I., Novosad, V., Padin, S., Pan, Z., Pearson, J., Posada, C. M., Rahlin, A., Ruhl, J. E., Saunders, L. J., Sayre, J. T., Shirley, I., Shirokoff, E., Smecher, G., Sobrin, J. A., Stan, L., Stark, A. A., Story, K. T., Suzuki, A., Tang, Q. Y., Thompson, K. L., Tucker, C., Vale, L. R., Vanderlinde, K., Vieira, J. D., Wang, G., Whitehorn, N., Yefremenko, V., Yoon, K. W., and Young, M. R., "Tuning SPT-3G Transition-Edge-Sensor Electrical Properties with a Four-Layer Ti-Au-Ti-Au Thin-Film Stack," *Journal of Low Temperature Physics* (Apr. 2018).

[30] Posada, C. M., Ade, P. A. R., Anderson, A. J., Avva, J., Ahmed, Z., Arnold, K. S., Austermann, J., Bender, A. N., Benson, B. A., Bleem, L., Byrum, K., Carlstrom, J. E., Carter, F. W., Chang, C., Cho, H.-M., Cukierman, A., Czaplewski, D. A., Ding, J., Divan, R. N. S., de Haan, T., Dobbs, M., Dutcher, D., Everett, W., Gannon, R. N., Guyser, R. J., Halverson, N. W., Harrington, N. L., Hattori, K., Henning, J. W., Hilton, G. C., Holzapfel, W. L., Huang, N., Irwin, K. D., Jeong, O., Khaire, T., Korman, M., Kubik, D. L., Kuo, C.-L., Lee, A. T., Leitch, E. M., Lendinez Escudero, S., Meyer, S. S., Miller, C. S., Montgomery, J., Nadolski, A., Natoli, T. J., Nguyen, H., Novosad, V., Padin, S., Pan, Z., Pearson, J. E., Rahlin, A., Reichardt, C. L., Ruhl, J. E., Saliwanchik, B., Shirley, I., Sayre, J. T., Shariff, J. A., Shirokoff, E. D., Stan, L., Stark, A. A., Sobrin, J., Story, K., Suzuki, A., Tang, Q. Y., Thakur, R. B., Thompson, K. L., Tucker, C. E., Vanderlinde, K., Vieira, J. D., Wang, G., Whitehorn, N., Yefremenko, V., and Yoon, K. W., "Large arrays of dual-polarized multichroic TES detectors for CMB measurements with the SPT-3G receiver," in [*Millimeter, Submillimeter, and Far-Infrared Detectors and Instrumentation for Astronomy VIII*], *Proc. SPIE* **9914**, 991417 (July 2016).

[31] Ding, J., Ade, P. A. R., Anderson, A. J., Avva, J., Ahmed, Z., Arnold, K., Austermann, J. E., Bender, A. N., Benson, B. A., Bleem, L. E., Byrum, K., Carlstrom, J. E., Carter, F. W., Chang, C. L., Cho, H. M., Cliche, J. F., Cukierman, A., Czaplewski, D., Divan, R., de Haan, T., Dobbs, M. A., Dutcher, D., Everett, W., Gilbert, A., Gannon, R., Guyser, R., Halverson, N. W., Harrington, N. L., Hattori, K., Henning, J. W., Hilton, G. C., Holzapfel, W. L., Hubmayr, J., Huang, N., Irwin, K. D., Jeong, O., Khaire, T., Kubik, D., Kuo, C. L., Lee, A. T., Leitch, E. M., Meyer, S. S., Miller, C. S., Montgomery, J., Nadolski, A., Natoli, T., Nguyen, H., Novosad, V., Padin, S., Pan, Z., Pearson, J., Posada, C. M., Rahlin, A., Reichardt, C. L., Ruhl, J. E., Saliwanchik, B. R., Sayre, J. T., Shariff, J. A., Shirley, I., Shirokoff, E., Smecher, G., Sobrin, J., Stan, L., Stark, A. A., Story, K., Suzuki, A., Tang, Q. Y., Thakur, R. B., Thompson, K. L., Tucker, C., Vanderlinde, K., Vieira, J. D., Wang, G., Whitehorn, N., Wu, W. L. K., Yefremenko, V., and Yoon, K. W., "Optimization of Transition Edge Sensor Arrays for Cosmic Microwave Background Observations With the South Pole Telescope," *IEEE Transactions on Applied Superconductivity* **27**, 2639378 (June 2017).

[32] Posada, C. M., Ade, P. A. R., Ahmed, Z., Anderson, A. J., Austermann, J. E., Avva, J. S., Thakur, R. B., Bender, A. N., Benson, B. A., Carlstrom, J. E., Carter, F. W., Cecil, T., Chang, C. L., Cliche, J. F., Cukierman, A., Denison, E. V., de Haan, T., Ding, J., Divan, R., Dobbs, M. A., Dutcher, D., Everett, W., Foster, A., Gannon, R. N., Gilbert, A., Groh, J. C., Halverson, N. W., Harke-Hosemann, A. H., Harrington, N. L., Henning, J. W., Hilton, G. C., Holzapfel, W. L., Huang, N., Irwin, K. D., Jeong, O. B., Jonas, M., Khaire, T., Kofman, A. M., Korman, M., Kubik, D., Kuhlmann, S., Kuo, C. L., Lee, A. T., Lowitz, A. E., Meyer, S. S., Michalik, D., Miller, C. S., Montgomery, J., Nadolski, A., Natoli, T., Nguyen, H., Noble, G. I., Novosad, V., Padin, S., Pan, Z., Pearson, J., Rahlin, A., Ruhl, J. E., Saunders, L. J., Sayre, J. T., Shirley, I., Shirokoff, E., Smecher, G., Sobrin, J. A., Stan, L., Stark, A. A., Story, K. T., Suzuki, A., Tang, Q. Y., Thompson, K. L., Tucker, C., Vale, L. R., Vanderlinde, K., Vieira, J. D., Wang, G., Whitehorn, N., Yefremenko, V., Yoon, K. W., and Young, M. R., "Fabrication of Detector Arrays for the SPT-3G Receiver," *Journal of Low Temperature Physics* (May 2018).

[33] Ding, J., Ade, P. A. R., Ahmed, Z.and Anderson, A. J., Austermann, J. E., Avva, J. S.and Thakur, R. B., Bender, A. N.and Benson, B. A., Carlstrom, J. E., Carter, F. W.and Cecil, T., Chang, C. L., Cliche, J. F.,

Cukierman, A., Denison, E. V., de Haan, T., Divan, R., Dobbs, M. A., Dutcher, D., Everett, W., Foster, A., Gannon, R. N., Gilbert, A., Groh, J. C., Halverson, N. W., Harke-Hosemann, A. H., Harrington, N. L., Henning, J. W., Hilton, G. C., Holzapfel, W. L., Huang, N., Irwin, K. D., Jeong, O. B., Jonas, M., Khaire, T., Kofman, A. M., Korman, M., Kubik, D., Kuhlmann, S., Kuo, C. L., Lee, A. T., Lowitz, A. E., Meyer, S. S., Michalik, D., Miller, C. S., Montgomery, J., Nadolski, A., Natoli, T., Nguyen, H., Noble, G. I., Novosad, V., Padin, S., Pan, Z., Pearson, J., Posada, C. M., Rahlin, A., Ruhl, J. E., Saunders, L. J., Sayre, J. T., Shirley, I., Shirokoff, E., Smecher, G., Sobrin, J. A., Stan, L., Stark, A. A., Story, K. T., Suzuki, A., Tang, Q. Y., Thompson, K. L., Tucker, C., Vale, L. R., Vanderlinde, K., Vieira, J. D., Wang, G., Whitehorn, N., Yefremenko, V.and Yoon, K. W., and Young, M. R., "Thermal links and microstrip transmission lines in spt-3g bolometers," *Journal of Low Temperature Physics* (Jun 2018).

[34] Dutcher, D. and et al., "Characterization and performance of the second-year SPT-3G focal plane," *Proc. SPIE* (2018).

[35] Dobbs, M. A., Lueker, M., Aird, K. A., Bender, A. N., Benson, B. A., Bleem, L. E., Carlstrom, J. E., Chang, C. L., Cho, H.-M., Clarke, J., Crawford, T. M., Crites, A. T., Flanigan, D. I., de Haan, T., George, E. M., Halverson, N. W., Holzapfel, W. L., Hrubes, J. D., Johnson, B. R., Joseph, J., Keisler, R., Kennedy, J., Kermish, Z., Lanting, T. M., Lee, A. T., Leitch, E. M., Luong-Van, D., McMahon, J. J., Mehl, J., Meyer, S. S., Montroy, T. E., Padin, S., Plagge, T., Pryke, C., Richards, P. L., Ruhl, J. E., Schaffer, K. K., Schwan, D., Shirokoff, E., Spieler, H. G., Staniszewski, Z., Stark, A. A., Vanderlinde, K., Vieira, J. D., Vu, C., Westbrook, B., and Williamson, R., "Frequency multiplexed superconducting quantum interference device readout of large bolometer arrays for cosmic microwave background measurements," *Review of Scientific Instruments* **83**, 073113 (July 2012).

[36] Bender, A. N., Cliche, J.-F., de Haan, T., Dobbs, M. A., Gilbert, A. J., Montgomery, J., Rowlands, N., Smecher, G. M., Smith, K., and Wilson, A., "Digital frequency domain multiplexing readout electronics for the next generation of millimeter telescopes," in [*Millimeter, Submillimeter, and Far-Infrared Detectors and Instrumentation for Astronomy VII*], *Proc. SPIE* **9153**, 91531A (July 2014).

[37] Bender, A. N., Ade, P. A. R., Anderson, A. J., Avva, J., Ahmed, Z., Arnold, K., Austermann, J. E., Basu Thakur, R., Benson, B. A., Bleem, L. E., Byrum, K., Carlstrom, J. E., Carter, F. W., Chang, C. L., Cho, H. M., Cliche, J. F., Crawford, T. M., Cukierman, A., Czaplewski, D. A., Ding, J., Divan, R., de Haan, T., Dobbs, M. A., Dutcher, D., Everett, W., Gilbert, A., Groh, J. C., Guyser, R., Halverson, N. W., Harke-Hosemann, A., Harrington, N. L., Hattori, K., Henning, J. W., Hilton, G. C., Holzapfel, W. L., Huang, N., Irwin, K. D., Jeong, O., Khaire, T., Korman, M., Kubik, D., Kuo, C. L., Lee, A. T., Leitch, E. M., Lendinez, S., Meyer, S. S., Miller, C. S., Montgomery, J., Nadolski, A., Natoli, T., Nguyen, H., Novosad, V., Padin, S., Pan, Z., Pearson, J., Posada, C. M., Rahlin, A., Reichardt, C. L., Ruhl, J. E., Saliwanchik, B. R., Sayre, J. T., Shariff, J. A., Shirley, I., Shirokoff, E., Smecher, G., Sobrin, J., Stan, L., Stark, A. A., Story, K., Suzuki, A., Tang, Q. Y., Thompson, K. L., Tucker, C., Vanderlinde, K., Vieira, J. D., Wang, G., Whitehorn, N., Yefremenko, V., and Yoon, K. W., "Integrated performance of a frequency domain multiplexing readout in the SPT-3G receiver," in [*Millimeter, Submillimeter, and Far-Infrared Detectors and Instrumentation for Astronomy VIII*], *Proc. SPIE* **9914**, 99141D (July 2016).

[38] Huber, M. E., Neil, P. A., Benson, R. G., Burns, D. A., Corey, A. F., Flynn, C. S., Kitaygorodskaya, Y., Massihzadeh, O., Martinis, J. M., and Hilton, G. C., "Dc squid series array amplifiers with 120 mhz bandwidth (corrected)," *IEEE Transactions on Applied Superconductivity* **11**, 4048–4053 (Jun 2001).

[39] de Haan, T., Smecher, G., and Dobbs, M., "Improved performance of TES bolometers using digital feedback," in [*Society of Photo-Optical Instrumentation Engineers (SPIE) Conference Series*], *Society of Photo-Optical Instrumentation Engineers (SPIE) Conference Series* **8452** (Sept. 2012).

[40] Rotermund, K., Barch, B., Chapman, S., Hattori, K., Lee, A., Palaio, N., Shirley, I., Suzuki, A., and Tran, C., "Planar Lithographed Superconducting LC Resonators for Frequency-Domain Multiplexed Readout Systems," *Journal of Low Temperature Physics* **184**, 486–491 (July 2016).

[41] Avva, J. S., Ade, P. A. R., Ahmed, Z., Anderson, A. J., Austermann, J. E., Thakur, R. Basuand Barron, D., Bender, A. N., Benson, B. A., Carlstrom, J. E., Carter, F. W., Cecil, T., Chang, C. L., Cliche, J. F., Cukierman, A., Denison, E. V., de Haan, T., Ding, J., Dobbs, M. A., Dutcher, D., Elleflot, T., Everett, W., Foster, A., Gannon, R. N., Gilbert, A., Groh, J. C., Halverson, N. W., Harke-Hosemann, A. H., Harrington, N. L., Hasegawa, M., Hattori, K., Henning, J. W., Hilton, G. C., Holzapfel, W. L., Hori, Y., Huang, N.,

Irwin, K. D., Jeong, O. B., Jonas, M., Khaire, T., Kofman, A. M., Korman, M., Kubik, D., Kuhlmann, S., Kuo, C. L., Lee, A. T., Lowitz, A. E., Meyer, S. S., Montgomery, J., Nadolski, A., Natoli, T., Nguyen, H., Nishino, H., Noble, G. I., Novosad, V., Padin, S., Pan, Z., Pearson, J., Posada, C. M., Rahlin, A., Rotermund, K., Ruhl, J. E., Saunders, L. J., Sayre, J. T., Shirley, I., Shirokoff, E., Smecher, G., Sobrin, J. A., Stark, A. A., Story, K. T., Suzuki, A., Tang, Q. Y., Thompson, K. L., Tucker, C., Vale, L. R., Vanderlinde, K., Vieira, J. D., Wang, G., Whitehorn, N., Yefremenko, V., Yoon, K. W., and Young, M. R., "Design and assembly of spt-3g cold readout hardware," *Journal of Low Temperature Physics* (May 2018).

[42] Montgomery, J., *Development of Multiplexed Bolometer Readout Electronics for mm-wave Space Astronomy*, Master's thesis, McGill University (2015).

[43] Sobrin, J. and et al., "Design and Characterization of the SPT-3G Receiver," *Proc. SPIE* (2018).

[44] George, E. M., Ade, P., Aird, K. A., Austermann, J. E., Beall, J. A., Becker, D., Bender, A., Benson, B. A., Bleem, L. E., Britton, J., Carlstrom, J. E., Chang, C. L., Chiang, H. C., Cho, H.-M., Crawford, T. M., Crites, A. T., Datesman, A., de Haan, T., Dobbs, M. A., Everett, W., Ewall-Wice, A., Halverson, N. W., Harrington, N., Henning, J. W., Hilton, G. C., Holzapfel, W. L., Hoover, S., Huang, N., Hubmayr, J., Irwin, K. D., Karfunkle, M., Keisler, R., Kennedy, J., Lee, A. T., Leitch, E., Li, D., Lueker, M., Marrone, D. P., McMahon, J. J., Mehl, J., Meyer, S. S., Montgomery, J., Montroy, T. E., Nagy, J., Natoli, T., Nibarger, J. P., Niemack, M. D., Novosad, V., Padin, S., Pryke, C., Reichardt, C. L., Ruhl, J. E., Saliwanchik, B. R., Sayre, J. T., Schaffer, K. K., Shirokoff, E., Story, K., Tucker, C., Vanderlinde, K., Vieira, J. D., Wang, G., Williamson, R., Yefremenko, V., Yoon, K. W., and Young, E., "Performance and on-sky optical characterization of the SPTpol instrument," in [*Millimeter, Submillimeter, and Far-Infrared Detectors and Instrumentation for Astronomy VI*], *Proc. SPIE* **8452**, 84521F (Sept. 2012).

[45] BICEP2 Collaboration, Ade, P. A. R., Aikin, R. W., Amiri, M., Barkats, D., Benton, S. J., Bischoff, C. A., Bock, J. J., Brevik, J. A., Buder, I., Bullock, E., Davis, G., Day, P. K., Dowell, C. D., Duband, L., Filippini, J. P., Fliescher, S., Golwala, S. R., Halpern, M., Hasselfield, M., Hildebrandt, S. R., Hilton, G. C., Irwin, K. D., Karkare, K. S., Kaufman, J. P., Keating, B. G., Kernasovskiy, S. A., Kovac, J. M., Kuo, C. L., Leitch, E. M., Llombart, N., Lueker, M., Netterfield, C. B., Nguyen, H. T., O'Brient, R., Ogburn, IV, R. W., Orlando, A., Pryke, C., Reintsema, C. D., Richter, S., Schwarz, R., Sheehy, C. D., Staniszewski, Z. K., Story, K. T., Sudiwala, R. V., Teply, G. P., Tolan, J. E., Turner, A. D., Vieregg, A. G., Wilson, P., Wong, C. L., and Yoon, K. W., "BICEP2. II. Experiment and three-year Data Set," *ApJ* **792**, 62 (Sept. 2014).

[46] Abbott, T. M. C., Abdalla, F. B., Allam, S., Amara, A., Annis, J., Asorey, J., Avila, S., Ballester, O., Banerji, M., Barkhouse, W., Baruah, L., Baumer, M., Bechtol, K., Becker, M. R., Benoit-Lévy, A., Bernstein, G. M., Bertin, E., Blazek, J., Bocquet, S., Brooks, D., Brout, D., Buckley-Geer, E., Burke, D. L., Busti, V., Campisano, R., Cardiel-Sas, L., arnero Rosell, A. C., Carrasco Kind, M., Carretero, J., Castander, F. J., Cawthon, R., Chang, C., Conselice, C., Costa, G., Crocce, M., Cunha, C. E., D'Andrea, C. B., da Costa, L. N., Das, R., Daues, G., Davis, T. M., Davis, C., De Vicente, J., DePoy, D. L., DeRose, J., Desai, S., Diehl, H. T., Dietrich, J. P., Dodelson, S., Doel, P., Drlica-Wagner, A., Eifler, T. F., Elliott, A. E., Evrard, A. E., Farahi, A., Fausti Neto, A., Fernandez, E., Finley, D. A., Fitzpatrick, M., Flaugher, B., Foley, R. J., Fosalba, P., Friedel, D. N., Frieman, J., García-Bellido, J., Gaz tanaga, E., Gerdes, D. W., Giannantonio, T., Gill, M. S. S., Glazebrook, K., Goldstein, D. A., Gower, M., Gruen, D., Gruendl, R. A., Gschwend, J., Gupta, R. R., Gutierrez, G., Hamilton, S., Hartley, W. G., Hinton, S. R., Hislop, J. M., Hollowood, D., Honscheid, K., Hoyle, B., Huterer, D., Jain, B., James, D. J., Jeltema, T., Johnson, M. W. G., Johnson, M. D., Juneau, S., Kacpr zak, T., Kent, S., Khullar, G., Klein, M., Kovacs, A., Koziol, A. M. G., Krause, E., Kremin, A., Kron, R., Kuehn, K., Kuhlmann, S., Kuropatkin, N., Lahav, O., Lasker, J., Li, T. S., Li, R. T., Liddle, A. R., Lima, M., Lin, H., López-Reyes, P., MacCrann, N., Maia, M. A. G., Maloney, J. D., Manera, M., March, M., Marriner, J., Marshall, J. L., Martini, P., McClintock, T., McKay, T., McMahon, R. G., Melchior, P., Menanteau, F., Miller, C. J., Miquel, R., Mohr, J. J., Morganson, E., Mould, J., Neilsen, E., Nichol, R. C., Nidever, D., Nikutta, R., Nogueira, F., Nord, B., Nugent, P., Nunes, L., Ogando, R. L. C., Old, L., Olsen, K., Pace, A. B., Palmese, A., Paz-Chinchón, F., Peiris, H. V., Percival, W. J., Petravick, D., Plazas, A. A., Poh, J., Pond, C., Por redon, A., Pujol, A., Refregier, A., Reil, K., Ricker, P. M., Rollins, R. P., Romer, A. K., Roodman, A., Rooney, P., Ross, A. J., Rykoff, E. S., Sako, M., Sanchez, E., Sanchez, M. L., Santiago, B., Saro, A., Scarpine, V., Scolnic, D., Scott, A., Serrano, S., Sevilla-Noarbe, I., Sheldon,

E., Shipp, N., Silveira, M. L., Smith, R. C., Smith, J. A., Smith, M., Soares-Santos, M., Sobre ira, F., Song, J., Stebbins, A., Suchyta, E., Sullivan, M., Swanson, M. E. C., Tarle, G., Thaler, J., Thomas, D., Thomas, R. C., Troxel, M. A., Tucker, D. L., Vikram, V., Vivas, A. K., Wal ker, A. R., Wechsler, R. H., Weller, J., Wester, W., Wolf, R. C., Wu, H., Yanny, B., Zenteno, A., Zhang, Y., and Zuntz, J., "The Dark Energy Survey Data Release 1," *ArXiv e-prints* (Jan. 2018).

[47] Schlegel, D. J., Finkbeiner, D. P., and Davis, M., "Maps of Dust Infrared Emission for Use in Estimation of Reddening and Cosmic Microwave Background Radiation Foregrounds," *ApJ* **500**, 525–553 (June 1998).

[48] Planck Collaboration, Aghanim, N., Akrami, Y., Ashdown, M., Aumont, J., Baccigalupi, C., Ballardini, M., Banday, A. J., Barreiro, R. B., Bartolo, N., Basak, S., Battye, R., Benabed, K., Bernard, J.-P., Bersanelli, M., Bielewicz, P., Bock, J. J., Bond, J. R., Borrill, J., Bouchet, F. R., Boulanger, F., Bucher, M., Burigana, C., Butler, R. C., Calabrese, E., Cardoso, J.-F., Carron, J., Challinor, A., Chiang, H. C., Chluba, J., Colombo, L. P. L., Combet, C., Contreras, D., Crill, B. P., Cuttaia, F., de Bernardis, P., de Zotti, G., Delabrouille, J., Delouis, J.-M., Di Valentino, E., Diego, J. M., Doré, O., Douspis, M., Ducout, A., Dupac, X., Dusini, S., Efstathiou, G., Elsner, F., Enßlin, T. A., Eriksen, H. K., Fantaye, Y., Farhang, M., Fergusson, J., Fernandez-Cobos, R., Finelli, F., Forastieri, F., Frailis, M., Franceschi, E., Frolov, A., Galeotta, S., Galli, S., Ganga, K., Génova-Santos, R. T., Gerbino, M., Ghosh, T., González-Nuevo, J., Górski, K. M., Gratton, S., Gruppuso, A., Gudmundsson, J. E., Hamann, J., Handley, W., Herranz, D., Hivon, E., Huang, Z., Jaffe, A. H., Jones, W. C., Karakci, A., Keihänen, E., Keskitalo, R., Kiiveri, K., Kim, J., Kisner, T. S., Knox, L., Krachmalnicoff, N., Kunz, M., Kurki-Suonio, H., Lagache, G., Lamarre, J.-M., Lasenby, A., Lattanzi, M., Lawrence, C. R., Le Jeune, M., Lemos, P., Lesgourgues, J., Levrier, F., Lewis, A., Liguori, M., Lilje, P. B., Lilley, M., Lindholm, V., López-Caniego, M., Lubin, P. M., Ma, Y.-Z., Macías-Pérez, J. F., Maggio, G., Maino, D., Mandolesi, N., Mangilli, A., Marcos-Caballero, A., Maris, M., Martin, P. G., Martinelli, M., Martínez-González, E., Matarrese, S., Mauri, N., McEwen, J. D., Meinhold, P. R., Melchiorri, A., Mennella, A., Migliaccio, M., Millea, M., Mitra, S., Miville-Deschênes, M.-A., Molinari, D., Montier, L., Morgante, G., Moss, A., Natoli, P., Nørgaard-Nielsen, H. U., Pagano, L., Paoletti, D., Partridge, B., Patanchon, G., Peiris, H. V., Perrotta, F., Pettorino, V., Piacentini, F., Polastri, L., Polenta, G., Puget, J.-L., Rachen, J. P., Reinecke, M., Remazeilles, M., Renzi, A., Rocha, G., Rosset, C., Roudier, G., Rubiño-Martín, J. A., Ruiz-Granados, B., Salvati, L., Sandri, M., Savelainen, M., Scott, D., Shellard, E. P. S., Sirignano, C., Sirri, G., Spencer, L. D., Sunyaev, R., Suur-Uski, A.-S., Tauber, J. A., Tavagnacco, D., Tenti, M., Toffolatti, L., Tomasi, M., Trombetti, T., Valenziano, L., Valiviita, J., Van Tent, B., Vibert, L., Vielva, P., Villa, F., Vittorio, N., Wandelt, B. D., Wehus, I. K., White, M., White, S. D. M., Zacchei, A., and Zonca, A., "Planck 2018 results. VI. Cosmological parameters," *ArXiv e-prints* (July 2018).

[49] Louis, T., Grace, E., Hasselfield, M., Lungu, M., Maurin, L., Addison, G. E., Ade, P. A. R., Aiola, S., Allison, R., Amiri, M., Angile, E., Battaglia, N., Beall, J. A., de Bernardis, F., Bond, J. R., Britton, J., Calabrese, E., Cho, H.-m., Choi, S. K., Coughlin, K., Crichton, D., Crowley, K., Datta, R., Devlin, M. J., Dicker, S. R., Dunkley, J., Dünner, R., Ferraro, S., Fox, A. E., Gallardo, P., Gralla, M., Halpern, M., Henderson, S., Hill, J. C., Hilton, G. C., Hilton, M., Hincks, A. D., Hlozek, R., Ho, S. P. P., Huang, Z., Hubmayr, J., Huffenberger, K. M., Hughes, J. P., Infante, L., Irwin, K., Muya Kasanda, S., Klein, J., Koopman, B., Kosowsky, A., Li, D., Madhavacheril, M., Marriage, T. A., McMahon, J., Menanteau, F., Moodley, K., Munson, C., Naess, S., Nati, F., Newburgh, L., Nibarger, J., Niemack, M. D., Nolta, M. R., Nuñez, C., Page, L. A., Pappas, C., Partridge, B., Rojas, F., Schaan, E., Schmitt, B. L., Sehgal, N., Sherwin, B. D., Sievers, J., Simon, S., Spergel, D. N., Staggs, S. T., Switzer, E. R., Thornton, R., Trac, H., Treu, J., Tucker, C., Van Engelen, A., Ward, J. T., and Wollack, E. J., "The Atacama Cosmology Telescope: two-season ACTPol spectra and parameters," *J. Cosmology Astropart. Phys.* **6**, 031 (June 2017).

[50] POLARBEAR Collaboration, Ade, P. A. R., Aguilar, M., Akiba, Y., Arnold, K., Baccigalupi, C., Barron, D., Beck, D., Bianchini, F., Boettger, D., Borrill, J., Chapman, S., Chinone, Y., Crowley, K., Cukierman, A., Dünner, R., Dobbs, M., Ducout, A., Elleflot, T., Errard, J., Fabbian, G., Feeney, S. M., Feng, C., Fujino, T., Galitzki, N., Gilbert, A., Goeckner-Wald, N., Groh, J. C., Hall, G., Halverson, N., Hamada, T., Hasegawa, M., Hazumi, M., Hill, C. A., Howe, L., Inoue, Y., Jaehnig, G., Jaffe, A. H., Jeong, O., Kaneko, D., Katayama, N., Keating, B., Keskitalo, R., Kisner, T., Krachmalnicoff, N., Kusaka, A., Le Jeune, M., Lee, A. T., Leitch, E. M., Leon, D., Linder, E., Lowry, L., Matsuda, F., Matsumura, T., Minami, Y., Montgomery, J., Navaroli, M., Nishino, H., Paar, H., Peloton, J., Pham, A. T. P., Poletti, D., Puglisi, G., Reichardt, C. L., Richards,

P. L., Ross, C., Segawa, Y., Sherwin, B. D., Silva-Feaver, M., Siritanasak, P., Stebor, N., Stompor, R., Suzuki, A., Tajima, O., Takakura, S., Takatori, S., Tanabe, D., Teply, G. P., Tomaru, T., Tucker, C., Whitehorn, N., and Zahn, A., "A Measurement of the Cosmic Microwave Background B-mode Polarization Power Spectrum at Subdegree Scales from Two Years of polarbear Data," *ApJ* **848**, 121 (Oct. 2017).

[51] Keisler, R., Hoover, S., Harrington, N., Henning, J. W., Ade, P. A. R., Aird, K. A., Austermann, J. E., Beall, J. A., Bender, A. N., Benson, B. A., Bleem, L. E., Carlstrom, J. E., Chang, C. L., Chiang, H. C., Cho, H.-M., Citron, R., Crawford, T. M., Crites, A. T., de Haan, T., Dobbs, M. A., Everett, W., Gallicchio, J., Gao, J., George, E. M., Gilbert, A., Halverson, N. W., Hanson, D., Hilton, G. C., Holder, G. P., Holzapfel, W. L., Hou, Z., Hrubes, J. D., Huang, N., Hubmayr, J., Irwin, K. D., Knox, L., Lee, A. T., Leitch, E. M., Li, D., Luong-Van, D., Marrone, D. P., McMahon, J. J., Mehl, J., Meyer, S. S., Mocanu, L., Natoli, T., Nibarger, J. P., Novosad, V., Padin, S., Pryke, C., Reichardt, C. L., Ruhl, J. E., Saliwanchik, B. R., Sayre, J. T., Schaffer, K. K., Shirokoff, E., Smecher, G., Stark, A. A., Story, K. T., Tucker, C., Vanderlinde, K., Vieira, J. D., Wang, G., Whitehorn, N., Yefremenko, V., and Zahn, O., "Measurements of Sub-degree B-mode Polarization in the Cosmic Microwave Background from 100 Square Degrees of SPTpol Data," *ApJ* **807**, 151 (July 2015).

[52] Planck Collaboration, Aghanim, N., Akrami, Y., Ashdown, M., Aumont, J., Baccigalupi, C., Ballardini, M., Banday, A. J., Barreiro, R. B., Bartolo, N., Basak, S., Benabed, K., Bernard, J.-P., Bersanelli, M., Bielewicz, P., Bock, J. J., Bond, J. R., Borrill, J., Bouchet, F. R., Boulanger, F., Bucher, M., Burigana, C., Calabrese, E., Cardoso, J.-F., Carron, J., Challinor, A., Chiang, H. C., Colombo, L. P. L., Combet, C., Crill, B. P., Cuttaia, F., de Bernardis, P., de Zotti, G., Delabrouille, J., Di Valentino, E., Diego, J. M., Doré, O., Douspis, M., Ducout, A., Dupac, X., Efstathiou, G., Elsner, F., Enßlin, T. A., Eriksen, H. K., Fantaye, Y., Fernandez-Cobos, R., Forastieri, F., Frailis, M., Fraisse, A. A., Franceschi, E., Frolov, A., Galeotta, S., Galli, S., Ganga, K., Génova-Santos, R. T., Gerbino, M., Ghosh, T., González-Nuevo, J., Górski, K. M., Gratton, S., Gruppuso, A., Gudmundsson, J. E., Hamann, J., Handley, W., Hansen, F. K., Herranz, D., Hivon, E., Huang, Z., Jaffe, A. H., Jones, W. C., Karakci, A., Keihänen, E., Keskitalo, R., Kiiveri, K., Kim, J., Knox, L., Krachmalnicoff, N., Kunz, M., Kurki-Suonio, H., Lagache, G., Lamarre, J.-M., Lasenby, A., Lattanzi, M., Lawrence, C. R., Le Jeune, M., Levrier, F., Lewis, A., Liguori, M., Lilje, P. B., Lindholm, V., López-Caniego, M., Lubin, P. M., Ma, Y.-Z., Macías-Pérez, J. F., Maggio, G., Maino, D., Mandolesi, N., Mangilli, A., Marcos-Caballero, A., Maris, M., Martin, P. G., Martínez-González, E., Matarrese, S., Mauri, N., McEwen, J. D., Melchiorri, A., Mennella, A., Migliaccio, M., Miville-Deschênes, M.-A., Molinari, D., Moneti, A., Montier, L., Morgante, G., Moss, A., Natoli, P., Pagano, L., Paoletti, D., Partridge, B., Patanchon, G., Perrotta, F., Pettorino, V., Piacentini, F., Polastri, L., Polenta, G., Puget, J.-L., Rachen, J. P., Reinecke, M., Remazeilles, M., Renzi, A., Rocha, G., Rosset, C., Roudier, G., Rubiño-Martín, J. A., Ruiz-Granados, B., Salvati, L., Sandri, M., Savelainen, M., Scott, D., Sirignano, C., Sunyaev, R., Suur-Uski, A.-S., Tauber, J. A., Tavagnacco, D., Tenti, M., Toffolatti, L., Tomasi, M., Trombetti, T., Valiviita, J., Van Tent, B., Vielva, P., Villa, F., Vittorio, N., Wandelt, B. D., Wehus, I. K., White, M., White, S. D. M., Zacchei, A., and Zonca, A., "Planck 2018 results. VIII. Gravitational lensing," *ArXiv e-prints* (July 2018).

[53] Sherwin, B. D., van Engelen, A., Sehgal, N., Madhavacheril, M., Addison, G. E., Aiola, S., Allison, R., Battaglia, N., Becker, D. T., Beall, J. A., Bond, J. R., Calabrese, E., Datta, R., Devlin, M. J., Dünner, R., Dunkley, J., Fox, A. E., Gallardo, P., Halpern, M., Hasselfield, M., Henderson, S., Hill, J. C., Hilton, G. C., Hubmayr, J., Hughes, J. P., Hincks, A. D., Hlozek, R., Huffenberger, K. M., Koopman, B., Kosowsky, A., Louis, T., Maurin, L., McMahon, J., Moodley, K., Naess, S., Nati, F., Newburgh, L., Niemack, M. D., Page, L. A., Sievers, J., Spergel, D. N., Staggs, S. T., Thornton, R. J., Van Lanen, J., Vavagiakis, E., and Wollack, E. J., "Two-season Atacama Cosmology Telescope polarimeter lensing power spectrum," *Phys. Rev. D* **95**, 123529 (June 2017).